JOURNAL OF MATERIALS SCIENCE 29 (1994) 294–323

Review
Structure and plastic deformation of polyethylene

L. LIN*, A. S. ARGON‡
Massachusetts Institute of Technology, Cambridge, MA 02139, USA

A review is given of the structure of semi-crystalline polymers and the mechanisms of plastic deformation in them. High-density polyethylene (HDPE) is taken as the specific example because of the large number of detailed studies performed on this material. The early findings are also compared and contrasted with very recent detailed large-strain deformation studies and computer simulations of deformation-induced texture development in HDPE.

1. Introduction

Polymers represent an important class of materials which have now become ubiquitous in application in modern life. Among these, the semi-crystalline polymers, as a sub-set, such as high-density polyethylene, nylon and polyethylene terephthalate, are of particular technological interest because of their remarkable deformability and toughness that permit them to undergo very large permanent strains resulting in highly anisotropic properties. These properties have been exploited not only in the production of high-modulus fibres, as precursors to carbon fibres, but also in more or less extensively textured form for synthetic fibres used in a multitude of woven and non-woven products.

The understanding of the basic mechanism of plastic deformation of these materials has been a subject of intense interest for at least the past three decades. The subject underwent intense research in the 1960s and 1970s starting with the molecular microstructure, the crystallization behaviour, the semi-crystalline morphology, and the mechanism of plastic deformation at the scale of crystalline lamellae. While the early investigations of plastic deformation, utilizing diffraction techniques and transmission electron microscopy, have been most imaginative and fruitful, they remained largely on the observational level and lacked the quantitative approach necessary for more general application to three-dimensional inhomogeneous deformation problems. In addition, these investigations suffered from the restriction that they were mostly in the usual tensile mode and were often derived from thin-film experiments lacking the constraints of more general deformation in bulk and being subject to many interesting but irrelevant deformation artefacts. To rectify these deficiencies, a comprehensive investigation was recently initiated into semi-crystalline polymers involving both extensive new experimental studies (mostly in compression and shear flow) and detailed computer simulations of large-strain deformation processes that lead to anisotropic texture development. These were carried out mainly in high-density polyethylene (HDPE) but also in nylon 6, polyethylene terephthalate and even in isotactic polystyrene. The experimental investigations by Argon and co-workers [1–11] and the associated computer simulation of plastic flow in semi-crystalline polymers by Parks and associates [12–15] have been and are being published elsewhere. They shed a new and more consistent light on the complex deformation process. In the preparation of the above-cited new investigations, we have performed an extensive review of much of the previous work on the structure of semi-crystalline polymers and the mechanisms of plastic flow in them, with particular emphasis on polyethylene which has been the most intensively researched material. The present communication is the result of this review. In this review, we have abstained from commenting much on the mechanisms of crystallization which we have decided are still too contentious and controversial to include. The interested reader should consult the proceedings of a recent international conference on the subject [16].

In the first part of our review covering structure and morphology of undeformed polyethylene, we strove to give our best assessment of the more or less generally accepted facts that are essential to understand and describe the mechanisms of plastic deformation. These mechanisms have been reviewed in the second half of this communication. In both the structure and the deformation mechanisms review, we have presented only a partial picture of the existing information that we considered most relevant. In this we have sometimes presented competing and contradictory reports by different investigators, but have in many cases also added our evaluations based on our view on

* *Present address*: E. I. du Pont de Nemours & Co., Marshall Laboratories, Philadelphia, PA 19146, USA.
‡ To whom all correspondence should be directed.

0022–2461

consistency with modern concepts of micro-mechanics and mechanisms of inelastic deformation, derived largely from the new investigations cited above.

The mechanics of inelastic deformation of heterogeneous media is presently undergoing intense developments from a mechanistic point of view, and the processes which occur in semicrystalline polymers represent a particularly challenging assignment. It is in view of this that we have decided to publish the present review, in the hope that it will stimulate further development in the understanding of the behaviour of these complex but very important materials.

2. Structure and morphology of undeformed polyethylene

In understanding the mechanical behaviour of a material, the structure and morphology are the most important starting considerations. They determine the possible behaviour patterns of the material. The variety in the microscopic structure and morphology influences the differences in properties of materials. In the past several decades much effort has been expanded on the investigation of the structure and morphology of polymers and particularly polyethylene (PE). Several reviews on the structure and morphology of this material exist in the literature [17–19].

Research on the morphology of PE can be classified into two major categories: the solution-grown single crystals and the melt-crystallized spherulites in bulk. The former has provided much of the fundamental understanding of the nature of crystallization of long-chain polymers under nearly ideal conditions and the resulting structural features, while the latter has furnished information on the spatial packing of crystallites in the majority of practical situations. Clearly, these two growth products are different and represent two extreme ways of reaching the solid state for a chain polymer. Much effort has been devoted to relate and contrast the morphology and behaviour of these two extreme cases. In a complementary case, "chain-extended" or "extended-chain" PE crystals have been obtained under high pressure. In addition to forms of crystallization, the forms of disorder and crystal defects, which are abundant in semi-crystalline polymers and may play important roles in determining many aspects of their mechanical properties, have attracted a great deal of attention.

Here, only a part of the important discoveries, i.e. those closely related to the deformation behaviour of the material, will be discussed with the aim of developing an understanding of the structure and morphology as well as the deformation behaviour of polymeric materials in general.

2.1. Crystalline lamellae

Polyethylene lamellar single crystals can be obtained from solution [20–22]. The thickness of these lamellae ranges from 5 to 25 nm and the lateral dimensions from 1 to 50 μm. The crystals have an orthorhombic structure as shown in Fig. 1. The planar zigzag carbon chains of the PE molecules are parallel to the crystallographic c axis in the orthorhombic unit cell of the crystal. The C–H and C–C bonds in the main chain are covalent, and the neighbouring chains are held together by van der Waals interactions. This regularity of molecular packing forms a crystal in the conventional sense. Electron diffraction experiments [21, 23] have indicated that the molecular chains are always nearly perpendicular to the flat surfaces of the lamellae. Some detailed investigations [24], however, showed that the molecular chains can incline up to 30° with lamellar faces in some cases. Keller [21] was the first to conclude, from the fact that the molecular chains are essentially perpendicular to the lamellar surfaces, that the long chain molecules must be folded back and forth many times on a plane perpendicular to the lozenge surface of lamellae, since over 90% of the molecules are many times longer than the lamella thickness.

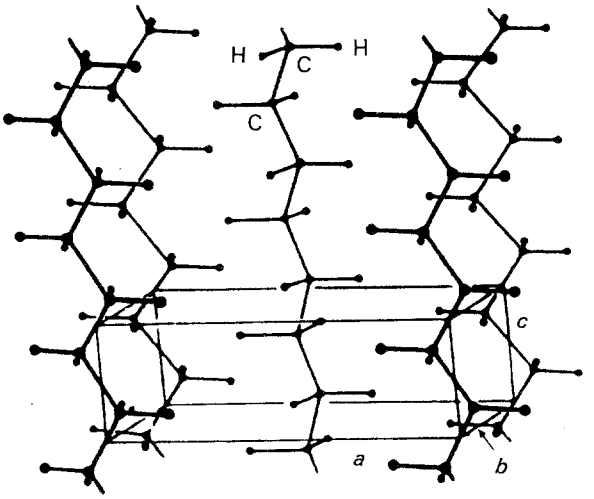

Figure 1 Perspective view of the orthorhombic crystal structure of polyethylene. $a = 0.74$ nm, $b = 0.493$ nm, $c = 0.254$ nm.

The lateral growth habit of PE crystals is an important feature studied in the solution-grown crystals. Well-formed PE single crystals are lozenge-shaped. The crystallographic a axis of the unit cell was found to be parallel to the long diagonal of the lozenge as shown in Fig. 2a [21]. The lamellar lozenge crystals are known to have a {1 1 0} fold plane in each of the four sectors of the lozenge [23, 25–27]. The four {1 1 0} faces of lamellar single crystals are often truncated along {1 0 0} faces (Fig. 2b) [25, 28, 29]. Detailed investigations [24, 30] have indicated that the truncation faces are often curved. The degree of truncation has been characterized by ratios A/B, A/C and x/y, and angles θ and φ, as defined in Fig. 2c. It was found that the ratios increase with increasing crystallization temperature or concentration of solution, or decreasing molecular weight [24, 31–33].

Sectored lamellae grown from dilute solution are usually not planar, but form hollow pyramids which readily collapse into a regularly pleated shape when pressed against a planar surface [25, 34]. Such non-planar features account for most of the cracks and pleats observed in solution-grown single crystals examined subsequently on flat surfaces [29, 35, 36]. The existence of non-planar growth shapes has been

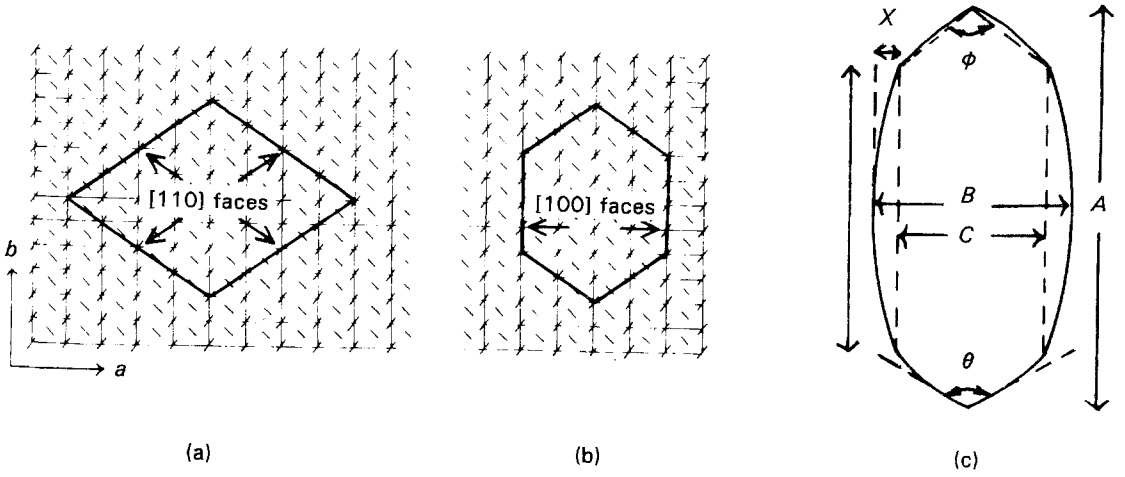

Figure 2 Schematic representation of polyethylene single crystals [30]: (a) lozenge shape, (b) truncation along {1 0 0} planes; (c) curved truncation along nominal {1 0 0} planes.

attributed [19, 36, 37] to either the presence of regular staggering of bulky molecular chain folds, or a slight buckling associated with a unit-cell distortion due to the folds, or both.

2.2. Spherulites

The spherulite is the most prevalent morphology in melt-crystallized bulk material. The size of spherulites generally depends upon the degree of undercooling. Under the usual growth conditions, spherulites are of the order of 100 μm in diameter. When fully impinged, the boundaries of spherulites are usually straight. This would follow if all nuclei had formed nearly simultaneously with a uniform radial growth rate.

It has been well established [38, 39] that the lamellae in a spherulite are embedded in a matrix of amorphous material, that the lamellae grow out from a common central nucleus, and that they are often twisted about the radial directions of the spherulite in a cooperative manner where neighbouring lamellae sympathetically twist with the same pitch and orientation. This is schematically illustrated in Fig. 3. According to several investigators [40–42] the pitch of twist increases with increasing crystallization temperature. The reason for the lamellar twisting has not been fully resolved. Moreover, the close packing of lamellae in spherulites cannot be rigorously described by topological models of full (monotonical) twists. Although an alternating arrangement of right- and left-hand partial twists of each lamella along their radial direction in spherulites has been suggested in conformity with the close packing [43], the majority of the lamellae observed do seem to be fully twisted.

The presence of lamellae has been identified in spherulites by electron microscopy [22], by small-angle X-ray scattering (SAXS) [44], and by controlled chemical degradation treatments [45, 46]. Through these, it has been established that the crystallographic *b* axes in lamellae are parallel to the radial growth directions in spherulites [38, 47], and that *a* axes and *c* axes are perpendicular to the corresponding radial directions. It has been shown by means of nitric acid digestion [45, 46] that chains are perpendicular to the

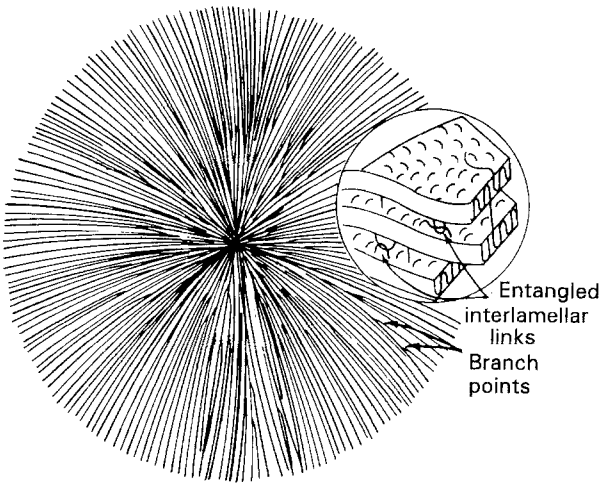

Figure 3 Schematic illustration of spherulite morphology [60].

large flat faces of the lamellae in spherulites. This leads to the same conclusion of crystallization by chain-folding, or at least chain association, for bulk material as was the case for solution-grown single crystals [46].

The lamellar profiles down the radii of spherulites (i.e. on projections along the *b* axis) are of three types [48, 49]: ridged sheets of alternating {2 0 1} facets, planar {2 0 1} sheets, and S-shaped sheets. The first-formed or dominant lamellae may have any of the three types of shapes, which lay down the framework of the morphological texture of a spherulite. The later-forming or subsidiary lamellae can only be ridged or planar, and they fill the already existing framework. Under practical crystallization conditions, the S-shape is the most prevalent form of lamellae. Consistent with the lamellar profiles, the molecular chains should incline to lamellar normals by an average angle of 35°, rather than being perpendicular to them.

The fold plane of the lamellae in spherulites was reported to be the {1 0 0} plane [50, 51], instead of the {1 1 0} plane in solution-grown single crystals. However, Allan and Bevis [52] have reported that the {1 1 0} plane is nearly always the preferred plane of slip and transformation shear in spherulites, which implies that this may also be the major fold plane. This

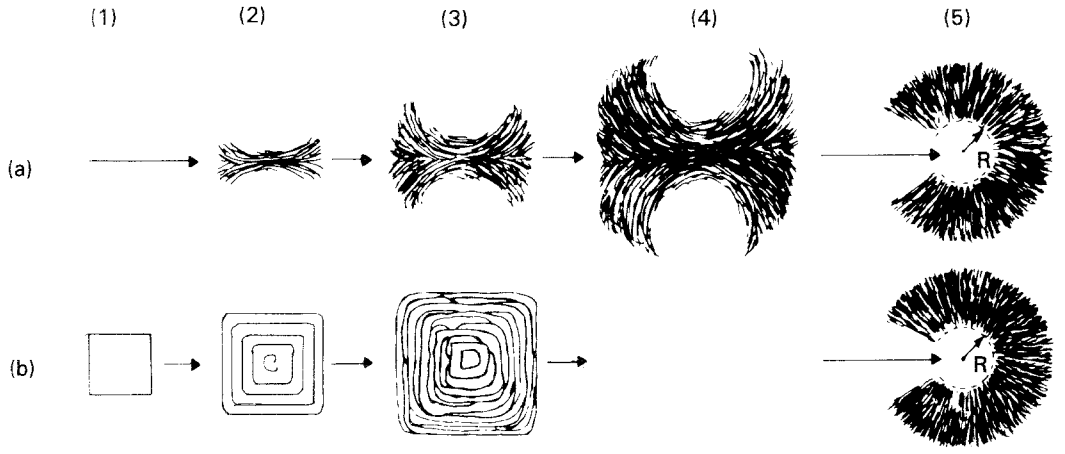

Figure 4 Schematic representation of successive stages in the development of a spherulite [19]: (a) edge-on view, (b) plan view.

early conclusion, however, is in conflict with more recent experiments which have firmly established that the {1 0 0} plane is the predominant slip plane [4]. It is interesting to note also that Kikuchi and Krimm [53] found that the fold plane can be transformed from {1 1 0} to {1 0 0} through a monoclinic phase during a martensitic shear deformation.

The development of spherulites is believed to be in several steps, as schematically illustrated in Fig. 4 [19]. First, a chain-folded monolayer single crystal fans out by non-crystallographic branching at its ends, and grows into sheaf-like multilayered crystals. Further radial growth of the intermediate lamellar aggregate leads to a spherically symmetric arrangement of ribbon-like, chain-folded lamellae. During the growth of spherulites, the lamellae may branch by developing adjacent shoots making small angles with each other to satisfy the necessary requirement of space filling. The remaining material between the branches may be solidified at a later stage in a following secondary crystallization process [54–56], or remain amorphous [57].

2.3. Relationship between crystals grown from solution and from the melt

Through examination of data on dissolution temperature (T_d) versus the reciprocal of the lamellar thickness ($1/l$) for solution-grown single crystals [58], and melting temperature (T_m) versus $1/l$ for melt-crystallized bulk PE [59], Hoffman *et al.* [60] related these two cases from the thermodynamics point of view. The relevant curves are shown in Fig. 5. Since the slope of the curves is proportional to the free energy of the fold surface, the fact that the lines are parallel indicates that the surface free energies are essentially the same for the lamellar single crystals and the bulk PE. This implies the thermodynamic similarity of the fold surface between the solution-grown and melt-crystallized PE crystals. The thermodynamic similarity provides a common ground for the two cases despite a large difference in morphology.

Fold lengths of crystals grown from the melt are much larger than those grown from solution. This phenomenon was explained by an isothermal thickening process of melt crystallization [61, 62]. Usually,

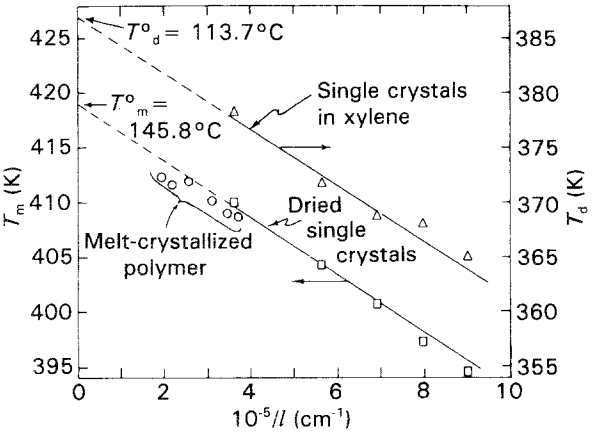

Figure 5 T_m versus $1/l$ and T_d versus $1/l$ plots for polyethylene, showing thermodynamic similarity of the fold surface in melt-crystallized and solution-grown crystals [60].

crystals grow at relatively lower temperature and lower undercooling from solution than from the melt. An overlap in the crystallization conditions in terms of both undercooling and absolute temperature has been achieved by raising the crystallization temperature for solution growth [30] and by lowering the accessible range of temperature for melt crystallization [63], so that comparison of the two cases becomes meaningful. Single crystals have been grown from solution in various solvents at temperatures in a range from 70 to 120 °C [64]. A specific dependence of fold length on undercooling has been found over the whole temperature range. Meanwhile, it has been found [62] by separating and accounting for the contribution of isothermal thickening that the initial fold lengths of lamellae from melt crystallization are much smaller than the lamellar thickness observed previously. Moreover, it has been found [65] that the initial fold lengths are determined by undercooling for both solution growth and melt crystallization, and that the subsequent thickening in melt crystallization is determined by the absolute temperature of the melt. Comparison of the initial fold lengths from solution and melt growth indicates now that they are substantially identical for the same undercooling conditions. In addition, the annealing behaviour has also been found to be similar between the lamellar single crystals and those of bulk material [66, 67].

Lamellae bounded by {1 1 0} and {1 0 0} planes and elongated in the *b* axis direction have been obtained from both solution growth [30] and melt crystallization [46]. A systematic study of the growth habit [30, 68] indicated that the elongation of solution-grown single crystals in the *b* axis direction with increasing solution concentration and crystallization temperature seems significant in explaining the spherulitic growth habit, i.e. the radial orientation of the *b* axes in spherulites of bulk PE.

By increasing the concentration in solution crystallization, a state corresponding to a pure melt state can be approached from solution continuously. Associated with this, the connection has been illustrated between spherulites and lamellae through the intermediate form of hedrites [69].

2.4. Crystals formed under pressure

Chain-extended (CE) PE crystals were first discovered in 1964 [70, 71]. In contrast with chain-folded crystals obtained at atmospheric pressure, which have thicknesses of about 20 nm, lamellae crystallized under a pressure of about 5 kbar (500 MPa) [71] were found to have thicknesses of up to 3 μm. Fracture surfaces of PE crystallized in this manner showed fine striations perpendicular to the broad faces of the lamellae. The chain-axis direction was identified to be parallel to these striations by electron diffraction and birefringence measurements. In this form, PE became quite brittle and had densities as high as 0.994 g cm^{-3} [70]. Moreover, in spite of the molecular-weight dependence, the lamellar thickness was found to be not limited by molecular length, i.e. under the right conditions molecules can be made to fit end-to-end inside one crystal to form a lamellar thickness several times larger than the extended molecular length [72, 73]. Lamellar crystals up to 40 μm in thickness have been obtained [72] for PE with $M_w = 50000$ in 200 h under conditions of 237 °C and 4.8 kbar (480 MPa).

During discussion of the crystallization mechanism of CE crystals and the origin of chain extension, an intermediate high-pressure hexagonal phase intervening in crystallization was proposed [74] and found [75] by Bassett and Turner, and also independently by Yasuniwa *et al.* [76]. Identification of the sequence was made by Bassett *et al.* [77] by means of a gasketed diamond-anvil cell. Accordingly, the CE crystallization was established to be a discontinuous change from the melt to an intermediate hexagonal phase, which then transformed from the hexagonal to the orthorhombic phase upon release of pressure and decrease of temperature. In this sequence, the average chain-axis direction was preserved in the transition between hexagonal and orthorhombic, indicating that the transformation must occur by shear in the *a*–*b* plane. The critical pressure and temperature for attaining the CE hexagonal phase of PE are about 3 kbar (300 MPa) and 235 °C [78].

From the thermal-stability point of view, Maeda *et al.* suggested [79] and later confirmed [80, 81] that there are two different kinds of extended-chain crystals, which they referred to as ordinary extended-chain crystal (OECC) and highly extended-chain crystal (HECC). For example, at a pressure of about 5 kbar (500 MPa), the crystallization and melting temperatures are 224 and 237 °C for OECC, but 228 and 244 °C for HECC, respectively. This difference apparently also exists in the hexagonal phase [82]. There are three pressure ranges proposed, in which the crystallization behaviour is different: (i) melt to chain-folded crystals directly at a pressure lower than 2 kbar (200 MPa), (ii) melt to chain-folded crystals and OECCs directly at pressure between 2 and 3.5 kbar (200 and 350 MPa), and finally (iii) above 3.5 kbar (350 MPa), from melt to a state consisting of low-melting point crystals (LMPCs), hexagonal OECCs and hexagonal HECCs, and then to LMPCs, orthorhombic OECCs and orthorhombic HECCs. The LMPCs may be chain-folded crystals and/or fully-extended-chain crystals of low molecular weight. When the crystallization pressure is higher than 4 kbar (400 MPa), process (iii) is found to be reversible [82], i.e. the melting route takes an orthorhombic solid through LMPCs and hexagonal OECCs and HECCs to melt.

2.5. Structural disorders and defects

Experimental evidence [17–19, 83] indicates that the material existing in a form other than perfect crystallites in polymers is substantial. The form of such material ranges from specific defects in the crystalline component to the general amorphous content. Although specific defects may be present within the crystalline component governing its plasticity, the general amorphous phase of the bulk polymer plays a predominant role in many aspects of the properties of semi-crystalline polymers. It is now generally agreed that the amorphous phase occurs predominantly at the fold surfaces [84] and that chain-folded lamellae consist of a central crystalline core sandwiched between two thin disordered layers [85]. The density of the central core is very nearly equal to the unit-cell density of perfect crystals. The disordered layers contain chain folds and have a lower density than the core. Various identifiable components of the disordered material include the "cilia" or chain ends at the fold surface, non-uniformities in the fold period, loose loops at adjacent and/or non-adjacent re-entry of molecules into the lamellae, and interfacial dislocation networks between lamellae.

2.5.1. Chain folding

An important outstanding matter is how the molecular chains are folded back into the lamellae from which they emerge. There are two extreme models for the re-entry of molecular chains into lamellae. One model (Fig. 6a) known as "random re-entry" with irregular chain folding [86, 87], also known as the switchboard model, allows molecules complete freedom in direction on the fold surfaces of the lamellae before re-entering the lamellae. The other model (Fig. 6b), known as "adjacent re-entry" with regular and systematic folding in a plane [21], requires all

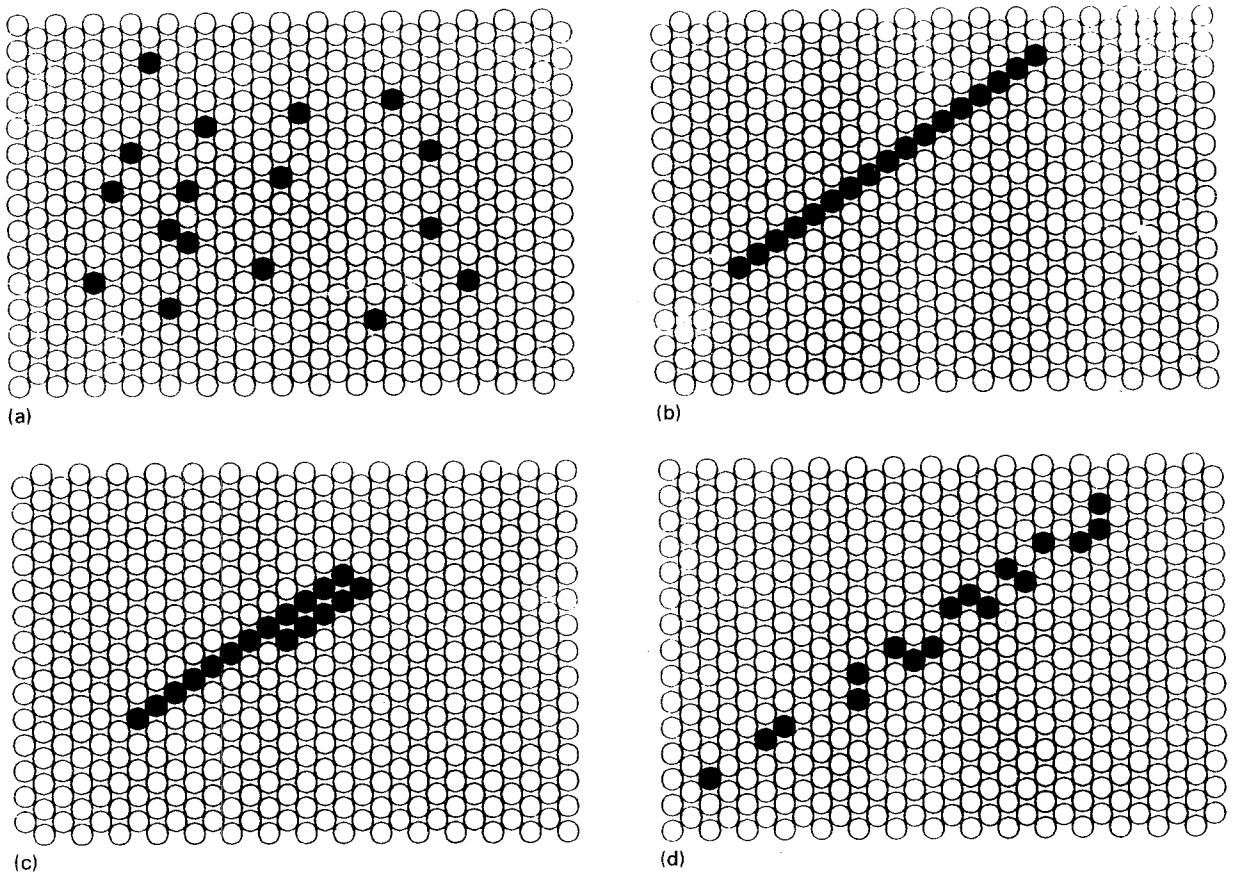

Figure 6 Models of stem re-entry for single crystal from solution [117]: (a) random fold model, (b) regular fold model, (c) regular fold model with superfolding, (d) stem-diluted model with superfolding.

molecules to tightly bend and re-enter the lamella at the nearest stem site. Which one of these models represents more closely the reality and governs the polymer morphology has been intensely debated from three points of view [88].

2.5.1.1. Relation of chain-folding models to properties. The specific morphology of the polymer should be able to account for most of the properties of the polymer. Alternatively, the properties can be used to test many features of the morphology through experiments. The earliest evidence supporting the regular fold model is the hollow pyramidal habit of sectored single crystals obtained from solution [35]. The pyramidal nature of unsupported lamellae requires crystallographically defined fold surfaces and regular fold staggering. In other words, the adjacent re-entry with regular folds of molecules is necessary for such well-defined fold surfaces and regular fold staggering. This argument, however, has been challenged by Mandelkern [89, 90], who cited Keller's report [18] that crystals displaying interfacial dislocations can also show sectorization. Although regular folding is the simplest interpretation of such a growth habit, other explanations may also be possible [90].

The density of the polymer is one of the most readily measurable properties. According to Frank [91, 92] the random fold model is incompatible with the assumption that the amorphous content of the polymer has lower density than does the crystalline core. This argument has been further developed in quantitative form by Guttman *et al.* [93]. They showed that more than two-thirds of re-entry should be adjacent. Mandelkern [89, 90], however, noted that about 15–20% of the chain units need to be in disordered conformations to account for a density with a value in the range of 0.96 to slightly greater than 0.97. But only 5% of the chain units is available if molecules return to lamellae according to the regular fold model.

Chain ends lying on the fold surfaces may also contribute to the disorder [94]. By reacting single crystals with ozone and examining them under infrared spectroscopy, Keller and Priest [95] have indeed found that about 90% of chain ends were excluded from the crystal lattice and lie on the crystal surfaces. Similar results were obtained by Witenhafer and Koeing [96] by using bromine in place of ozone. Occurrence of cilia (dangling molecule ends) on crystal surfaces has been shown more directly by Bank and Krimm [97] from their infrared spectra studies on single-crystal mats of blends of PE and deuterated PE. That the chain ends prefer to lie on the surfaces is probably because the excess free energy will be minimized as a result as internal crystal defects are avoided [98]. This may also be affected by minimization of chain overcrowding in the amorphous regions [99]. The extent of exclusion of chain ends from the interior of lamellae depends upon the distribution of molecular weight and crystallization conditions. As observed by Bassett [100], chain ends are found to be inside lamellae for conditions of rapid crystallization of polydisperse samples, while for slower crystallization of sharp fractions, chain ends become excluded from

lamellae. The conclusion reached by Keller and Priest [95] and Bank and Krimm [97] based on their infrared spectra studies, is that the cilia on the crystal surfaces account for a large fraction of the amorphous content for single crystals grown from solution.

Mandelkern [89, 90] proposed that the cilia of chain ends cannot contribute enough disorder to account for the density defect. His argument is based on the observation that the thickness of lamellae crystallized from a given solvent is independent of molecular chain length but depends solely upon the crystallization temperature when the molecular weight is greater than 1.5×10^4. Since the properties are invariant with molecular weight over a wide range, it must be concluded either that chain ends between lamellae have no important effect on properties, or possibly more correctly, that the structure of the amorphous layer between lamellae is unaffected by molecular weight over a wide range.

Random variations in fold length may cause the fold surface to roughen, i.e. become more disordered. Kinetic theories [101, 102] of crystallization predict that there must be considerable random variations in fold length. Detailed studies on selective degradation of PE single crystals with fuming nitric acid carried out by Keller *et al.* [103] have indicated a distribution of fold lengths. The variation in the excursion away from the lamellar surfaces of molecular segments making up the folds can be up to about 2 nm. From this Keller *et al.* [103] concluded that the random variations in the lengths of two folding segments must contribute substantially to the disorder. Keller [104] suggested, moreover, that the further the folds are situated from the central core, the looser they tend to be.

Krimm and co-workers [50, 105–108] have undertaken a series of studies using infrared spectra on mixed crystals of deuterated PE and hydrogenated PE. They interpreted the line-splitting modes in the mixed crystals as being caused by the specific arrangement of chain stems with predominantly regular folds on the crystal surfaces [50]. Mandelkern [90] has questioned the uniqueness of the interpretation and pointed out that such line splitting may be the result of phase separation between the different molecular species, which then may not give information on the nature of the fold pattern. The phase separation alone, however, would have resulted in too weak a signal [108]. Thus, the main findings by Krimm and Cheam [107] appear convincing: that folding with adjacent re-entry along $\{1\,1\,0\}$ planes predominates in the solution-grown crystals, and that in addition, there is a high probability that a molecule will fold back along itself on the next adjacent (1 1 0) plane. Subsequently, however, Jing and Krimm [108] showed that the folding behaviour of molecules is very different for the melt-crystallized PE, with a much lower (if any) extent of adjacent re-entry.

2.5.1.2. Molecular mobility considerations. To form a regularly folded morphology of crystals from a melt of polymer in which molecules randomly entangle one another, extensive disengagements and rearrangement of molecular chains are necessary. It is a point of general agreement that crystallization of a semi-crystalline polymer takes place under conditions far from thermodynamic equilibrium and is predominantly controlled by kinetic factors. The question is whether, in such kinetically controlled processes of crystallization, molecules have the ability and time to disengage and rearrange themselves to the regular form required in adjacent re-entry. This kinetic argument directly challenges the foundation of the regular fold model.

Flory and Yoon [109] estimated that the characteristic relaxation time was about 1 s for a complete rearrangement of a molecule of 900 nm length ($M_w = 10^5$) at 120 °C. However, the time to deposit the molecule in folded form at an average growth rate of 10^2 μm s^{-1} along the growth front should be within about 10^{-4} s. Thus, it is impossible for a molecule to disengage and rearrange fully to the regular fold form in the available time. They concluded that the highly entangled topological relationship of chains that exist in the melt must be largely retained in the semi-crystalline state of the solid.

The mobility problem has also been studied by Klein and Ball [110] and DiMarzio *et al.* [111]. They applied the reptation theory of DeGennes [112] to their calculation. Klein and Ball [110], in particular, have examined the dynamics of molecules crystallizing from a melt and found that the characteristic relaxation time of a PE segment of 50–100 monomer units is in the range of 10^{-7} to 10^{-6} s. From this they concluded, by comparing their results with deposition rates estimated from growth rates measured experimentally, that regular folding is indeed possible. DiMarzio *et al.* [111] developed a reptation theory to calculate the rate of reeling-in a molecule from the melt. They showed that the characteristic relaxation time is two to five orders of magnitude smaller than the one calculated by Flory and Yoon [109] so that the process is compatible with the observed growth rates. Therefore, these workers have concluded that the regular folding model is permissible on the ground of molecular mobility.

2.5.1.3. Small-angle neutron scattering studies. Because hydrogen and deuterium interact strongly with neutrons and have quite different scattering lengths, small-angle neutron scattering (SANS) permits the determination of molecular weight and radius of gyration, and hence morphological features of suitably labelled polymers. After the overcoming of two major experimental problems associated with SANS, related to the formation of voids of sub-micrometre dimensions between amorphous and crystalline regions and the segregation of tagged molecules into clusters during sample preparation, this technique has been used widely in studies of crystalline polymers in the solid state [113]. There are several comprehensive reviews concerning scattering theories, instrumentation and applications of SANS to polymer science [114–116].

On the issue regarding the nature of the fold surface, the SANS technique has been considered the most powerful tool at present to have provided new information. Sadler and Keller [117–119] found that in solution-grown single crystals, radii of gyration (R_g) are generally remarkably reduced and SANS results are consistent with the adjacent re-entry model. They also showed that the dependencies of R_g on molecular weight M_w are quite different for crystals grown from solution and from the melt. However, the experimental results for solution-grown crystals [119] have indicated that R_g is proportional to $M_w^{0.1}$ instead of M_w for $9 \times 10^4 < M_w < 18 \times 10^4$. This was interpreted as arising from "superfolding" of adjacent re-entry strips (Fig. 6c), developed when two chains on the same strip meet and continue to crystallize by folding a new strip parallel to and adjacent to the original one.

Yoon and Flory [120–122] calculated the absolute scattering intensities from single crystals for various models and showed that the adjacent re-entry model fails to fit the experimental curve by a factor of 2 to 3. They proposed a "stem-diluted superfolding" model (Fig. 6d) which is consistent with the experimental curves.

In the case of polymers crystallized from the melt, surprisingly, Schelten *et al.* [123] found that the radius of gyration of crystals in bulk material was similar to that found in the molten state. This led Flory and Yoon [109] to conclude that the random entanglements in the molten state must be largely conserved and concentrated in the amorphous regions during solidification.

It has been noted by Frank [92] that since the radius of gyration is essentially the square root of the ratio of the second to the zeroth moment of a distribution function, the value of R_g alone gives very limited information about conformational details of a molecule in space, although its invariance during crystallization certainly provides some information. This average number could indicate that a model is wrong, but cannot guarantee that another model is right. In fact many new models, which come from modifications of either the two extreme models of chain folding, satisfy the requirement that R_g substantially remain unchanged. For example, Guttman *et al.* [124] suggested a central cluster model and a variable cluster model. Both of these models fit the SANS data and have 60–80% of adjacent re-entries of chains.

In summary, it is clear that further research is necessary to develop a more complete understanding of the nature of chain folding of crystals solidified from the melt. Nevertheless, the available information strongly suggests that adjacent or nearly adjacent re-entry of molecular chains prevails in single crystals obtained from solution. In melt-grown crystals, however, the majority of evidence seems to favour much less chain folding as the required extraction of molecules from the melt and their addition to a crystal–melt interface in an orderly manner is likely to be quite imperfect.

2.5.2. Intercrystalline links

Regardless of the way in which molecules re-enter lamellae, it is widely accepted that there must be a sizable percentage of molecules that do not fold back into the same lamellae in polymers crystallized from the melt. In other words, it should be quite likely that a molecule does not only become part of a single lamella but also "snakes" out from one lamella into another or even from one spherulite to another. Such molecules bridging lamellae are termed "tie molecules". The molecular chains connecting different lamellae can form interlamellar links by associating into bundles.

The existence of tie molecules in bulk polymers was first proposed by Keith and Padden [42] to account for the mechanical behaviour of spherulites in PE. It is known that PE can undergo very large plastic strains when deformed under stress. A material composed of lamellae and spherulites without intercrystalline connections would be quite fragile and would be expected to fail at the interlamellar and interspherulitic boundaries at a much smaller stress than that observed.

There is direct evidence that significant concentrations of intercrystalline links exist in melt-crystallized polymers. Keith *et al.* [125, 126] crystallized two-dimensional spherulites of PE with a diluent of low molecular weight which does not change the growth mode. After the removal of the diluent by dissolution, intercrystalline links were revealed with electron microscopy. They found that the intercrystalline links are crystalline bundles with molecular chains parallel to the long axis of the links. This finding led them to conclude that an intercrystalline link is formed by crystallizing one molecule in two different lamellae simultaneously until it is drawn taut. Then these intercrystalline portions of such more stable taut molecules serve as a substrate for further crystallization of other molecules to form bundles. Evidence for the existence of intercrystalline links has also come from deformation studies [127–130] and thermal analysis [131].

Quantitative estimates of the fraction of tie molecules have been made by several investigators [124, 132–137]. Table I contains the available data. It is clear that the estimates based on mechanical properties are much lower than those by other methods. This discrepancy can be explained [133] by noting that tie molecules cannot share load equally due to the presence of molecular heterogeneities, length variations, and differences in the degree of tautness of tie molecules, so that a high stress concentration can occur on a portion of the taut tie molecules, producing a sequential rupture cascade much like the growth of a crack. Clearly, in the absence of information on the degree of load sharing between tie molecules, interpretation of mechanical properties will lead to underestimates of the fraction of tie molecules. The fraction estimated on the basis of mechanical properties actually considers only the active, taut tie molecules.

Distributions of chain lengths of tie molecules in the interlamellar regions were calculated theoretically by several investigators [138–140] to furnish a basis for better interpretation of mechanical properties. These calculations have established that only a small

TABLE I Estimated fraction of tie molecules

Method	Tie molecules (%)	References
Molecular weight analysis of samples treated with fuming nitric acid	5–30	[132]
To explain elastic modulus and tensile strength of drawn PE	1–4	[133]
To explain the anisotropy of the γ relaxation of drawn PE	0.26	[134]
To explain dynamic moduli based on mechanical two-phase model	1	[135]
SANS	4–8	[124]
SANS	12	[136]

fraction of the tie molecules are taut. According to the results of Popli and Roylance [140], the ratio of the mean length of the tie molecules to the thickness of amorphous layers is larger than a factor of 2.

2.5.3. Lamellar defects

As in most solids in bulk form, polymers contain a variety of defects in the crystalline regions. Many ideas and concepts of defects, which have been well developed for metallic and other inorganic crystalline materials, were introduced into the study of polymers. However, the long-chain nature of molecules of polymers introduces important constraints that modify such considerations markedly. Fig. 7 is a cartoon by Hosemann [141] giving a graphical catalogue of defects in a linear PE "paracrystal". The "paracrystal" is a concept used to describe an intermediate state between liquids and crystals. In addition to the usual point defects such as phonons, local charge defects, excitons, vacant lattice sites, interstitial atoms, and substitutional and interstitial single atoms, the lamellar crystals should contain more complex chain-packing defects such as chain ends, chain twist and kinks, dislocations, interfaces between different crystallographic forms, and finally amorphous matter [142]. Of these the latter six will be of particular interest to explain inelastic deformation mechanisms and ultimately fracture behaviour.

2.6. Quantitative structural models

Current understanding of polymer structures and properties is still largely at a phenomenological level, except in the case of the kinetic theories of crystallization. In spite of this, several investigators have given quantitative descriptions of the morphologies of semi-crystalline polymers. These, however, seem not to have attracted very much attention. Since such developments are of considerable use in understanding large-strain deformation in these materials, we review some prominent attempts below.

At the atomic level, computer models have been developed by Bacon and Geary [143] for theoretical analysis of crystal defects in PE. In their model, two assumptions were made for the problem to be tractable. One is that there are no intramolecular distortions, i.e. a molecule is only allowed rigid-body displacements and rotations. Another is that the molecules are straight and infinite in length, i.e. the fold surfaces are ignored. Intermolecular interactions in the model are described in terms of interatomic pair potentials. Based on this model, lattice parameters and elastic constants were calculated [143]; the structure and energy of stacking faults and coherent twin boundaries were studied [144]; and the core structure of dislocations in crystals was investigated [145].

Spherulites are usually composed of twisted lamellae growing radially as described in Section 2.2. Based on observations of spiral structure with two arms of spherulites, in the reflected-light microscopy and electron microscopy of replicated growth surfaces of PE bulk samples, Thornton and Predecki [146] idealized the lamellar structure of spherulites and gave two mathematical models of the lamellar stacking in spherulites. They assumed, for the sake of simplicity, that the entire spherulite was filled with lamellae twisted in the same sense. The structure of the spherulite centre, which would otherwise contain a topological singularity, occasional observed discontinuities in the spiral structure, and possible branching of lamellae, were all excluded. Under the assumption that the loci of points of a constant twist angle on lamellae form continuous spherical surfaces, Thornton and Predecki [146] have provided two possible models of spatial stacking of twisted lamellae, which are in general capable of describing the major features of the spherulite structure of PE.

Statistical equations describing spherulite growth and impingement in two and three dimensions have been developed by Piorkowska and Galeski [147] for any distribution of primary nuclei in space and time and their radial outward growth. Their formulae allow calculation of various distance distributions of boundary and inner points, from which the surface area of boundaries and the number of points belonging to more than three spherulites can be obtained for three-dimensionals tacking of spherulites (or boundary line length and the number of points belonging to more than two spherulites, for two-dimensional spherulites). It is also possible to simulate spherulite nucleation and growth in order to calculate size distributions and spherulite shapes [148].

3. Plastic deformation of polyethylene

Under increasing shear stress, the initial reversible elastic response of a solid eventually gives way to plastic behaviour. The plastic deformation of PE has been studied on different geometric scales. Some of the earlier findings were reviewed by Bowden and Young [149] and by Haudin [150]. Our discussion will proceed from the crystallographic scale to the spherulitic, and then to the macroscopic scale.

3.1. Deformation on the crystallographic scale

While the inelastic response of semi-crystalline PE at room temperature begins with deformation of the

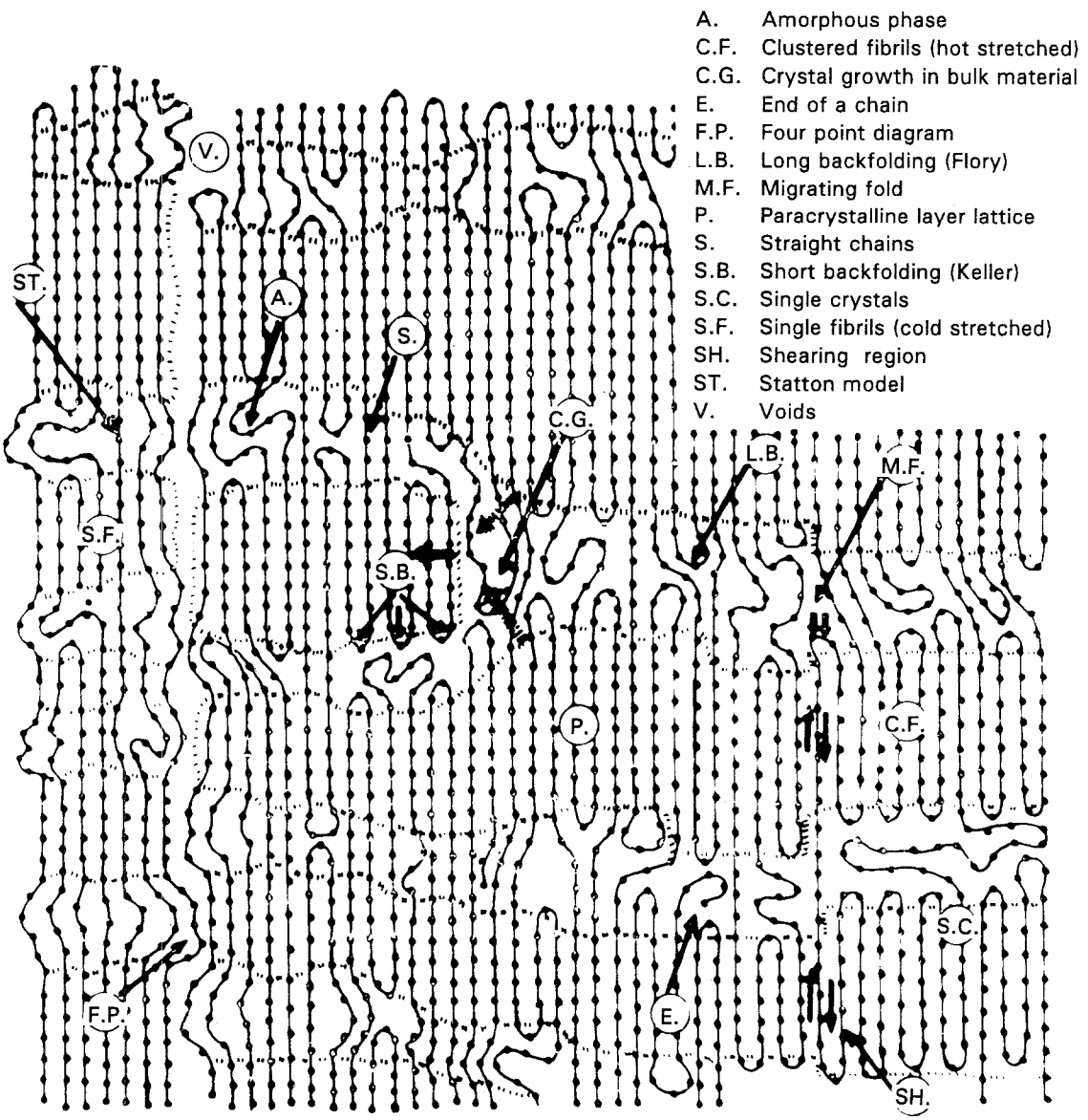

Figure 7 Schematic illustration of different types of defect in a linear polyethylene paracrystal [141].

amorphous component, this is rapidly exhausted and replaced by deformation of the crystalline lamellae by various crystallographic processes up to large plastic strains. Plastic deformation without chain unfolding or fracture occurs in many PE single crystals for tensile elongations up to at least 150% [151]. In bulk PE at very large strain in tensile deformation, internal stresses between inhomogeneously deforming component parts reach critical levels resulting in widespread cavitation, reduction of constraints and loss of compatibility. Following this cavitation, the chain-folded lamellar structure is discontinuously transformed into microfibrils. Such transformation, occurring in tensile extension and involving large-strain local drawing, made possible through the cavitation loss of constraints, is a very complex process. It has been studied first by Peterlin [152], who called it descriptively "micronecking". The full details of this deformation process have not been completely resolved. Recent experiments by Argon and co-workers [1–3] of large-strain plastic deformation of PE in plane strain compression, uniaxial compression and simple shear have shown that the cavitation process is a characteristic artefact of the tensile extension process and is inessential in achieving very large strains. Therefore, we will focus here on the details of the crystallographic mechanisms of straining and will de-emphasize micronecking.

The corresponding plastic deformation mechanisms in the crystallites involve predominantly crystallographic slip, but also to a lesser degree mechanical twinning and stress-induced martensitic transformations, which are quite similar to those occurring in many other inorganic types of crystalline material. In addition, intercrystalline deformation in the amorphous regions must continue to occur as crystalline deformation continues for reasons of compatibility. The plastic deformation mechanisms in the intercrystalline regions must be predominantly of a simple shear type. Some authors have assumed other mechanisms, such as interlamellar separation and lamella-stack rotation on the basis of some rare events.

3.1.1. Deformation by crystallographic slip

Slip is the dominant mode of plastic deformation of polymer crystals. If constraints imposed by the local neighbourhood permit, it can result in larger levels of

plastic strain than any of the other mechanisms. Crystallographic slip is characterized by two vectors, $(h\,k\,l)$ and $[u\,v\,w]$, that identify the "slip system". The vectors $(h\,k\,l)$ and $[u\,v\,w]$ represent the "slip plane" unit normal vector and the "slip direction" in the slip plane, respectively. When a critical resolved shear stress (CRSS), characteristic of the specific slip system, is reached on the slip plane in the slip direction, dislocation motion occurs on the slip plane and causes the two parts of the crystal separated by the plane to undergo a relative translation.

The long-chain nature of polymer molecules requires that the most preferred slip plane in polymer crystals contains the molecular chain. The PE chains can remain unbroken through very large deformations [153]. This means that the slip plane must be of the $\{h\,k\,0\}$ type for PE crystals. For a relatively large slip in a direction perpendicular to the chain direction (transverse slip) the slip planes are further restricted to the planes of chain folds, because slip in these planes will still not disrupt molecular folds on the crystal surfaces if the folds are of the adjacent re-entry type, as they would be in solution-grown crystals. In melt-grown crystals where adjacent re-entry and even chain folds are far less prevalent, the choice of planes for transverse slip is governed by more intrinsic properties of crystallographic planes governing dislocation mobility.

The shear strength of crystalline materials is in general much lower than the ideal shear strength of perfect crystals, and dislocations are responsible for this reduction.Thus, deformation by slip is usually governed by the resistance to the motion of dislocations on the slip planes. The character of the dislocation line is established by its Burgers vector. When the Burgers vector is parallel to the chain axis the deformation is called "chain slip", and when perpendicular it is called "transverse slip".

The presence of dislocations in polymer crystals was demonstrated from moiré fringes [87, 154–158] between lamellae, and from direct observation [159, 160] through contrast effects in dark-field electron microscopy. Various patterns of dislocations in PE were proposed by Frank *et al.* [161] and Keith and Passaglia [162], and were more extensively discussed by Predecki and Statton [163]. Fig. 8 illustrates four basic types governing both chain slip and transverse slip.

The existence of any type of dislocation in a crystal is governed first by minimum energy considerations, based on the line energy of the dislocation. Shadrake and Guiu [164, 165] calculated the line energies of straight dislocations of various types in anisotropic PE crystals of infinite extent. Their results are given in Table II in the order of increasing energy. It can be seen from the table that screw dislocations have generally lower line energies than edges. The screw dislocation along the chain direction possesses the lowest line energy.

Experimental results have shown that the shear resistances of oriented polymers in both the chain direction and the transverse direction depend upon normal stress acting across the shear planes [4, 8, 166–169]. Furthermore, this behaviour can be approximated by a linear relation of the type

$$\tau = \tau_0 - \mu_0 \sigma_n \qquad (1)$$

where τ_0 is the CRSS in the absence of any normal stress on the slip planes and μ_0 is called the normal stress sensitivity factor (NSSF). The CRSSes and NSSFs of the major deformation systems of PE and nylon 6 are listed in Table III. The above relation is known as the Coulomb yield criterion [170], and is found to be widely applicable to granular materials. This criterion is, however, rarely used in the plasticity of metal crystals since pressure dependence of yield is not prevalent for metallic materials at the usually relatively low levels of CRSS of these materials in comparison to their shear moduli. For semi-crystalline polymers, as in other polymers where the plastic resistance is a substantial fraction of the shear modulus, the normal stress (or pressure) dependence of yield is substantial. The normal stress dependence of the shear resistance was also reported for amorphous polymers [171–173].

The exact origins of the normal-stress dependence of the shear resistance or more generally the yield stress in polymers have not been fully understood. The long-chain nature of polymers or perhaps the large size of molecular repeat units is the principal differentiating feature of polymer crystals when compared with metal crystals. This is supported by the fact [174] that the out-of-plane C–H, N–H and C=O groups of nylon 6 crystals result in increased "roughness" of slip planes and are, no doubt, the principal cause of the larger normal-stress dependence of the slip resistance in that structure. That the critical shear stresses are usually a larger fraction of the elastic moduli in polymers than they are in metals is another reason for the high sensitivity of the shear resistance to normal stress of polymers.

In general, plastic deformation of a material is a thermally activated process [175]. Therefore, the mechanical properties are generally dependent on temperature and strain rate (time). The thermal activation involved in the microscopic mechanism, its stress dependence and its temperature and rate dependence, are of great importance in the study of the plastic behaviour of materials. In recent research [9], a simple shear experiment was developed specifically for studying the temperature and strain-rate dependences of crystallographic shear in highly textured polymers. This experiment provides a convenient way to directly measure the CRSS and other important quantities of the material without being disturbed by the normal stress dependence of these properties. Experiments were performed on the highly textured quasi-single crystalline nylon 6 under various conditions of temperature and strain rate. The results of the experiments show that the plastic shear resistance of the principal chain slip mechanism has a rather unique temperature dependence. Both the resolved shear stress and the flow stress at large strain have a very similar temperature dependence. While the elastic shear modulus of the highly textured material undergoes a very significant drop around 310 K due to an

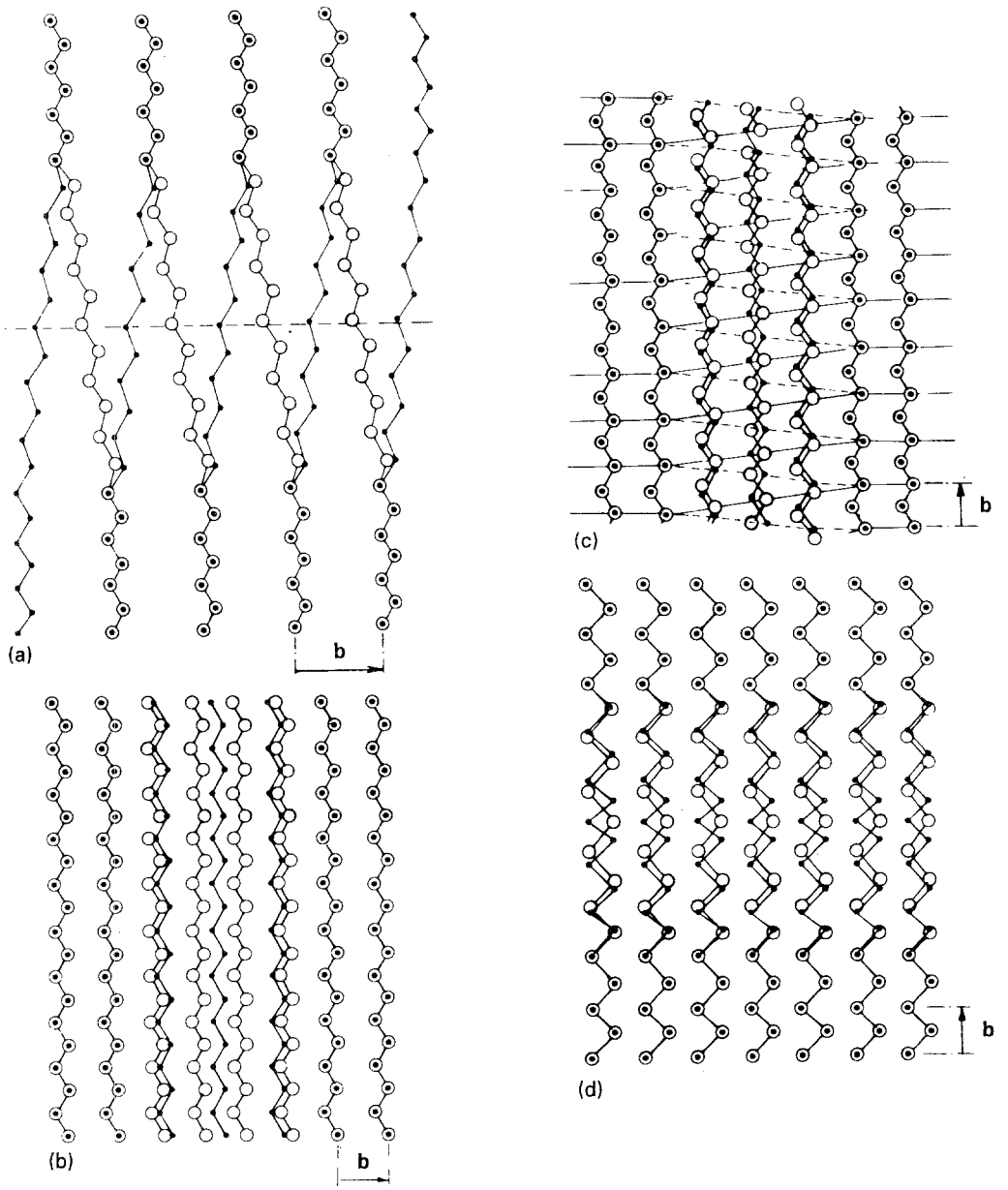

Figure 8 Models of dislocations in polyethylene [163]: (a) screw dislocation with a Burgers vector normal to the chain, (b) edge dislocation with a Burgers vector normal to the chain, (c) screw dislocation with a Burgers vector parallel to the chain, (d) edge dislocation with a Burgers vector parallel to the chain.

TABLE II Simple dislocations and their line energy factors [164]

Type	Dislocation line direction	Burgers vector[a]	Line energy Kb^2 (10^{-11} J m^{-1})	Associated slip system
1	[001]	[00c] (S)	9.59	(100) [001] or (010) [001]
2	[010]	[0b0] (S)	58.9	(100) [010]
3	[100]	[a00] (S)	69.6	(010) [100]
4	[001]	[0b0] (E)	82.0	(100) [010]
5	[010]	[00c] (E)	89.3	(100) [001]
6	[001]	[a00] (E)	137.2	(010) [100]
7	[100]	[00c] (E)	163.9	(010) [001]
8	[001]	[ab0] (E)	219.3	($\bar{b}a$0) [ab0]
9	[110]	[00c] (E)		(110) [001]
10	[110]	[ab0] (E)		($\bar{b}a$0) [ab0]

[a] S = screw dislocation, E = edge dislocation.

apparent glass transition in the amorphous component, there is no related discontinuity in the CRSS or in the flow stress with temperature change. Since the plastic resistance and the modulus are usually closely related, we must conclude that the actual plastic resistance of the amorphous material does not have much influence on the overall plastic resistance in later stages of deformation, which is apparently governed

TABLE III Critical resolved shear stresses and normal-stress sensitivity factors

Polymer	Slip system	τ_0 (MPa)	μ_0	Reference
PE	(100) [001]	7.2	0.11	[4]
	(010) [001]	15.6	0.20	
	(100) [010]	12.2	0.17	
Nylon 6	(001) [010]	16.2	0.13	[8]
	(100) [010]	23.2	0.28	
	(001) [100]	23.2	0.13	

primarily by the crystalline component. These outwardly conflicting observations are reconciled by a proposed new constitution of the textured material and its influence on the plastic resistance, discussed elsewhere [9].

Furthermore, by imposing sudden changes of strain rate on deforming samples in the simple shear experiments, very important quantities, principally the shear activation volume, were obtained for the material [9]. These quantities were examined and linked to a dislocation motion process affecting principally the crystalline component but negotiating through the amorphous component. The shear-stress dependence of the activation volume was determined to relate to the microstructure or morphology of the material through such a dislocation mechanism.

3.1.1.1. Chain slip. Theoretically, there are four types of dislocations that can result in chain slip (Types 1, 5, 7 and 9 in Table II). Because the [001] screw dislocation (Type 1) has the lowest line energy, it should be the preferred type in PE crystals. Because the Burgers vector in the chain direction is the shortest, glide along this direction may be the easiest. Thus, chain slip associated with the motion of dislocations of this type is taken as the most important crystallographic deformation mechanism.

In crystal plasticity, it has been well established that for single slip, the slip direction in crystals always rotates toward the tensile axis, or away from the compression axis. Kiho *et al.* [176] showed that the molecular chain of PE single crystals deposited on extensible substrates rotated and became tilted when the substrates were extended. Hay and Keller [177] found changes of molecular orientation from complete randomness to gradual alignment in the draw direction as a result of drawing in the bulk. Chain slip with molecular alignment was also clearly illustrated by Keller and Pope [178, 179] in deforming PE possessing "double texture" [180, 181] and "single texture" [182–185]. In addition, chain slip was identified by Stachurski and Ward [186] in small-strain dynamic modulus experiments with α-relaxation.

According to studies of slip traces on the surfaces of PE single crystals deformed upon Cu single-crystal substrates, Gleiter and Argon [187] suggested that chain slip could take place on any $\{hk0\}$ plane. Furthermore, they showed that chain slip was the only possible deformation activated at − 196 °C, although in the mode of forcing deformation that they used other forms of slip were distinctly not favoured.

Experiments revealed the existence of the (100) [001] slip system [1,4,177,188] and the (010) [001] slip system [1,4,177,169] for PE crystals, which can be interpreted as chain slip by the motion of screw or edge dislocations in the (100) and (010) planes, respectively. Experiments by Petermann and Gleiter [159] using transmission electron microscopy strongly support the above interpretation. When the (100) [001] system is activated, the chain axes will rotate about the *b* axis toward the tensile axis, while activity on the (010) [001] system produces rotation about the *a* axis. Hay and Keller [177] found that deformation took place first in the equatorial regions of PE spherulites, i.e. rotation of molecular chains around the *b* axis occurs more readily than around the *a* axis. This led them to conclude that (100) [001] slip was easier than (010) [001] slip, as noted earlier by Frank *et al.* [189] and recently re-confirmed by Bartczak *et al.* [4] by direct macroscopic measurements. The ease of (100) [001] slip may be due to the fact that the interplanar distance for the (100) planes is larger than for the (010) planes, but in any event it indicates that the plastic resistance of the (100) [001] system is the lowest.

Chain slip in the same type of planes can occur in two different ways to achieve the same macroscopic deformation [69, 190–192]. First, it could occur by fine slip, where a small amount of slip occurs equally on a large number of parallel planes [(Fig. 9a). Such deformation will result in a change of the angle between the molecular chain axis and the normal to the

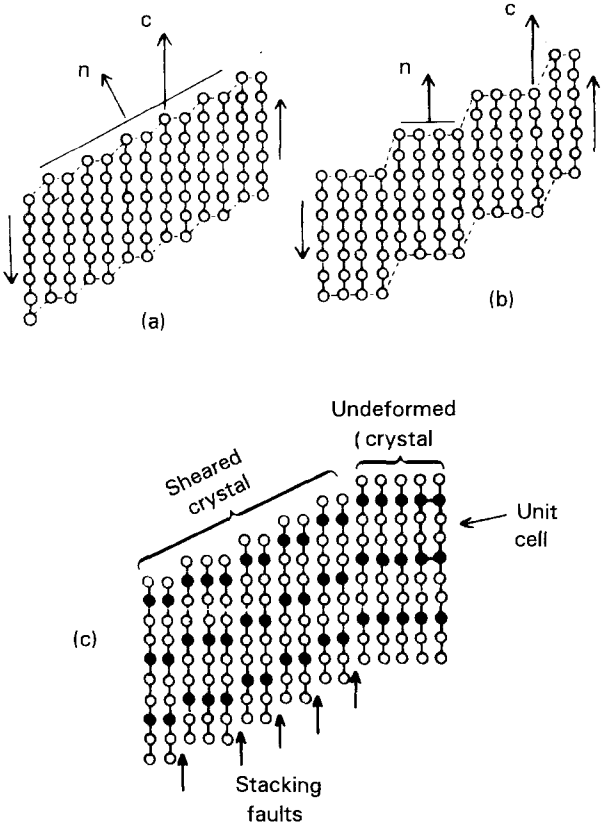

Figure 9 Schematic illustrations of different degrees of fineness of slip [149]: (a) fine slip, (b) coarser slip, (c) shearing of a lattice that has a large lattice translation vector in the chain direction by fine slip of partial dislocations.

lamellar surface. Second, coarse slip (or fibrillar slip) can occur by a large amount of slip on only a few parallel planes (Fig. 9b). The angle between the chain axis and this lamellar normal will not change during the deformation. These two types of slip are distinguishable because the direction of the chain axis and the lamellar normal are obtained from wide-angle X-ray diffraction and SAXS separately. According to Peterlin [152], microfibrils are the most important structural elements in drawn polymers. The corresponding deformation process for such microfibrillar structure would appear to be this type of coarse slip. Pope and Keller [178] found no evidence for coarse slip in deforming their textured PE samples at relatively low strains. Fine slip was reported to be the predominant mode of plastic deformation of oriented HDPE in compression [2, 169] and tension [190]. Hinton *et al.* [193] and Burnay *et al.* [192] found that coarse slip became more and more important with increasing strain. In addition, decrease of the angle between the tensile axis and chain direction could result in an increase of coarse slip [192]. Recent detailed studies of Galeski *et al.* [1] of large-strain deformation of HDPE in plane strain compression have shed new light on the nature of crystalline slip processes, furnishing new interpretations of these two different slip processes and indicating that coarse slip is a consequence of a local stretching instability in lamellae undergoing deformation by fine chain slip at a critical strain of 1.12.

It has been generally assumed that chain slip does not result in distortions of crystals having simple unit cells. This assumption was verified by Pope and Keller [178] for PE. However, chain slip in polymer crystals with large unit cells, such as nylons, can occur by partial dislocations with Burgers vectors less than the full lattice translation vector (Fig. 9c), such that the shapes of the unit cells are changed [191]. Such slip appears to require much lower applied stress, so it will occur preferentially, even though slip by partial dislocations should produce high-energy stacking faults or misfit layers; however, these appear to have low energy and do not inhibit this type of deformation.

Kink bands were observed frequently in oriented crystalline polymers, mainly during uniaxial compression [194–198], but also under tension [197], shear [199] and bending [200]. The principal mechanism involved in this type of deformation was found to be directly associated with organized chain slip, resulting in a form of crystallographic buckling. The concept of micro-buckling was proposed by Wu *et al.* [198] to interpret the deformation stability observed in PE under compression. A theoretical analysis led Pertsev and Vladimirov [201] to propose that kink band formation during plastic deformation of oriented polymers is related to the high elastic anisotropy of the material together with the associated plastic anisotropy. DeTeresa *et al.* [202] applied classical elastic instability theory to a solid composed of idealized polymer chains interacting with each other laterally, and calculated critical loads for chain buckling and hence the compressive strength of the material. They stated that the resistance of a single chain to buckling is governed by its bending stiffness, and that this resistance is, therefore, proportional to bond bending and torsional resistance, so that the compressive strength is proportional to either the shear modulus or the shear strength of a collection of molecular chains. Clearly, the specialized mechanisms of kinking referred to above have failed to take note of the fact that kinking by chain slip is a special case of the geometrical deformation instability treated generally by Frank and Stroh [203]. Moreover, kinking is also widely observed in aligned fibre composites where its critical stress for activation has been identified to be directly proportional to the interfibrillar shear resistance and inversely proportional to the angle of misorientation between the compression axis and the fibre direction [204]

3.1.1.2. Transverse slip. The transverse slip systems in PE crystals were studied by Frank *et al.* [161]. The closest packing direction for the transverse slip in PE crystals is the [0 1 0] direction, and then the [1 0 0] direction. Since the slip systems of (0 1 0) [1 0 0] and (1 0 0) [0 1 0] are orthogonal to one another, the resolved shear stress will always be the same. This implies that the (1 0 0) [0 1 0] system will always be activated first. In addition, the dislocations for the [0 1 0] slip direction should be easier to generate than the [1 0 0] slip direction, since this requires considerably lower line energies as seen in Table II.

Slip on the (1 1 0) planes was also reported. Some investigators have attributed major importance to it [52, 205]. Allan and Bevis [52] found that the main transverse slip system is of the $\{1\,1\,0\}\ \langle 1\,\bar{1}\,0\rangle$ type. Although the $\{1\,1\,0\}\ \langle 1\,\bar{1}\,0\rangle$ slip system involves a larger Burgers vector and activating dislocations on these planes may require a larger stress, unit dislocations on these planes may be able to dissociate into partial dislocations of the type $[a/2, b/2, \gamma]$ or $[a/2, b/2, -\gamma]$ [161]. These Burgers vectors are even shorter than that of the [0 1 0] dislocation, if γ is small, but their passage through the crystals should produce a high-energy stacking fault. In some instances there is some evidence that $\{1\,1\,0\}\ \langle 1\,\bar{1}\,0\rangle$ may be the best slip system available, e.g. in polar regions of spherulites [52]. In recent experiments on HDPE in plane strain compression, uniaxial compression and simple shear, evidence of $\{1\,1\,0\}\ \langle 1\,\bar{1}\,0\rangle$ slip activity was slight at best [2–4]. Moreover, attempts to directly measure the shear resistance of this system on highly textured quasi-single crystalline PE was not too successful because of earlier activity in several other competing systems [4]. For instance, $\{1\,1\,0\}$ twinning modes were reported to be strong competitors [149], but even these did not contribute substantially to the overall strain.

Chain slip and transverse slip can occur simultaneously on a common slip plane [169, 206]. Since the Burgers vector for chain slip is smaller than for any transverse slip, the CRSS of chain slip is lower, as discussed by Bowden and Young [149]. They showed that PE deformed by rolling acquired a texture with the [0 0 1] direction parallel to the rolling direction and the (1 0 0) plane perpendicular to the compression

direction before unloading. (When the material was unloaded, the above texture might change by twinning due to residual internal compressive stresses [180].) From crystal plasticity, this implies that the slip plane is [1 0 0] for both the chain slip direction (0 0 1) and the transverse slip direction [0 1 0], and that chain slip has a lower CRSS and is activated first.

3.1.1.3. Dislocation generation. In crystal plasticity, it is well established that the yield stress of crystals is controlled by the mobility of dislocations and their multiplication during deformation. To match the observed strain rate, dislocation sources are required to provide a high enough density of mobile dislocations at the applied stress level to replenish the dislocations that are stored or annihilated, to maintain a constant dislocation flux.

Predecki and Statton [207] showed from purely geometrical considerations that chain ends within the crystal lattice can produce both screw and edge dislocations, albeit as tight prismatic loops. Since chain ends that may be situated in PE crystals may occupy a volume fraction as high as 0.1 [95], such loops should be quite common. They further illustrated that a pair of chain ends can produce a dislocation loop with its Burgers vector perpendicular to the chain direction, and that the loop can act topologically as a Frank–Read source if these two chain ends become coupled [208]. However, there has been no experimental verification of the prismatic loops predicted by Predecki and Statton.

The mechanisms of dislocation generation in polymer crystals seem to be considerably different from those in metals because of the chain nature of molecules and the very small size, at least in one dimension, of crystallites of polymers in spherultic form. Peterson [209] has pointed out that the lamellar thickness is too small for Frank–Read sources to operate at a reasonable applied stress. This would also follow from the extremely small mesh length of the prismatic loops discussed above.

As stated above, the line tensions of straight dislocations with a variety of orientations were calculated by Shadrake and Guiu [164, 165]. They found, as is well known for isotropic solids, that the line tension of all screw dislocations in anisotropic PE is higher than that of the corresponding edges. The line tension of the [0 0 1] screw dislocations is, in fact, so high that these dislocations should have great difficulty in bowing out or bypassing any strong pinning points, but must advance in quasi-straight form. In other orientations the line tension is so low that effective conditions of negative line tension are possible, indicating that dislocations at such orientations are unstable under the action of very small internal stresses. Thus, the [0 0 1] dislocation responsible for the chain slip can only exist in a nearly pure screw orientation in nearly straight form and will not be able to multiply.

In order to explain the slip mechanism by dislocation motion, other alternatives for dislocation generation have to be found in addition to those initially present, such as chain ends in crystals. Peterson [209] proposed that thermal fluctuations, coupled with a large local shear stress, may provide a mechanism for the generation of screw dislocations from the edges of lamellar crystals of polymers in a mode of nucleation-controlled glide. He showed that the energy fluctuation required to produce a dislocation of 20 nm length from an edge of a lamella to a position from which it can expand under the usual levels of stress is only of the order of 1 eV because of the thinness of lamellar crystals and the low value of the longitudinal shear modulus. Thus, such a dislocation generation process should be energetically feasible in polymer crystals at room temperature.

This mechanism of dislocation generation was applied by Young [210] to interpret the variation of the CRSS of HDPE. Re-examining the Peterson mechanism, he found that the thermal energy fluctuation required for generation of a dislocation in a crystal of 20 nm thickness should be about 4 eV, and therefore should not be a likely process – at least in the initially conceived form. Thus, in order for this mechanism to operate, either the true value of the shear modulus C_{44} should be about one-quarter of that considered, or there should be at least some parts where the lamellar thickness at an edge is less than 5 nm, although the average thickness of the lamellae may still be 20 nm as indicated by SAXS. Later measurements [211–213] of the elastic constants C_{44} were indeed found to be a factor of 1.9–3.5 times lower than the value (C_{44} = 3.4 GPa) used by Young. Nevertheless, Young's analysis [210] indicates that the yield stress should depend directly upon the lamellar thickness in a certain range of thicknesses, if the yield stress is indeed governed by dislocation nucleation. The model used by Peterson [209] and Young [210] in the calculation of critical energies for formation of dislocations were for perfect chains in an isotropic elastic medium. Shadrake and Guiu [164, 165], on the other hand, took the anisotropy of PE crystals into account, and showed that the anisotropy further reduces the energy required for dislocation generation. In a recent simple shear study on textured nylon 6 by Lin and Argon [9], experimental results showed that the temperature sensitivities of the plastic resistance of major slip systems of the material are at least two orders of magnitude larger than those of crystalline materials, e.g. Zn and Cd [214]. The higher temperature dependence indicates that thermal fluctuations must play a much more important role in dislocation generation and multiplication in polymer crystals than in metallic crystals. In summary, all the above indicates that Peterson's model is quite credible, and is, most likely, one of the operating mechanisms governing the plastic shear resistance of lamellar crystals with distinct borders at the crystal–amorphous layer interface, as it is likely to be in the initial spherulitic morphology.

3.1.2. Mechanical twinning and stress-induced martensitic transformations

Mechanical twinning and stress-induced martensitic phase transformations are two additional modes of

deformation of crystallites. These two modes are important deformation mechanisms because they can potentially result in plastic deformation even if slip is geometrically unfavourable, and because they provide possibilities supplementary to slip. Wu *et al.* [215] found, by deforming PE single crystals on copper and NaCl single-crystal substrates, that the critical shear stresses for twinning and phase transformation in the *a–b* plane are lower than that for slip in the plane.

Again, the long-chain nature of polymer molecules determines that all twinning and martensitic phase transformations in PE will produce shear strains in the *a–b* plane, i.e. they should all be of the $\{hk0\}$ $\langle k\bar{h}0\rangle$ type. A theoretical geometrical framework for predicting modes of twinning and martensitic transformation in PE crystals has been established by Bevis and Crellin [216], from more general theories [217–219] of crystallographic shear transformations.

3.1.2.1. Mechanical twinning. The modes of twinning can be characterized by a plane K_1, called the twin plane (or the first invariant plane), which is common to both the deformed and the parent crystal structure (Fig. 10), and a direction η_1 lying in the K_1 plane, called the twin direction, which indicates the direction of uniform shear. There is a second undistorted but rotated plane K_2 (the second invariant plane). The angle between the normals of K_1 and K_2 changes from ϕ before shear to $\pi-\phi$ after shear. The twinning shear angle is $\pi-2\phi$, while the conventionally defined shear strain γ is $2\cot\phi$.

As a deformation mechanism in PE, twinning was first recognized by Frank *et al.* [161] to interpret plastic deformation processes in PE crystals. From symmetry considerations, the twinning modes were of the $\{3\,1\,0\}$ and $\{1\,1\,0\}$ types (referring to the twinning plane K_1), with both having twinning shear strains of $\gamma = 0.25$. Bevis and Crellin [216] systematically studied all possible modes of twinning that can occur in the PE crystal structure, and found shear strains for the $\{3\,1\,0\}$ and $\{1\,1\,0\}$ types to be the smallest of all that are possible. Allan *et al.* [220], furthermore, concluded from experimental observations that the $\{3\,1\,0\}$ and $\{1\,1\,0\}$ twinning modes are the only modes that become activated. The $\{3\,1\,0\}$ and $\{1\,1\,0\}$ twinning processes result in lattice rotations about the chain axis (the crystallographic c axis) of 55° and −67°, respectively.

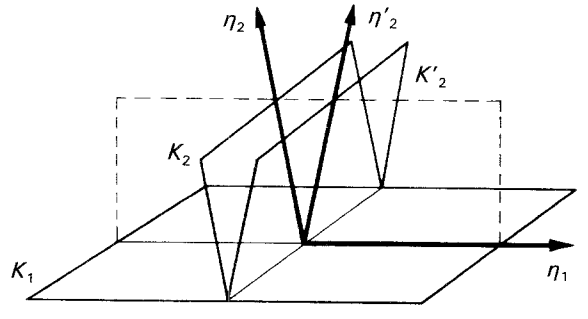

Figure 10 Schematic illustration of twin plane and twin direction [216].

Experimental work by many investigators [52, 151, 161, 206, 220–229] has indicated that in single crystals only the $\{1\,1\,0\}$ twinning mode occurs, and that in bulk materials the $\{1\,1\,0\}$ twinning mode always occurs before the $\{3\,1\,0\}$ twinning mode. Allan and Bevis [52, 229] studied deformation processes of spherulites in slowly melt-crystallized thin films of HDPE, and found that the fold planes are predominantly of the $\{1\,1\,0\}$ type and that the initial twinning process is $\{1\,1\,0\}$ twinning and not $\{3\,1\,0\}$ twinning. Furthermore, Preedy and Wheeler [228] showed that $\{1\,1\,0\}$ twinning occurs at relatively low stresses and that $\{3\,1\,0\}$ twinning occurs only under conditions of high strain during which the crystalline morphology is changed from lamellar to microfibrillar, when the state of internal stress is unclear. Structural details, particularly the chain folds, may affect the primary twinning mode [56, 151, 228, 229]. The preferred $\{1\,1\,0\}$ twinning is probably due to the constraint of the chain folds in the $\{1\,1\,0\}$ plane in addition to the fact that the shear strain is the smallest (as well as, most likely, the CRSS).

Shadrake and Guiu [164, 165] studied dislocation dissociations that might be involved in twinning and found that the dissociated dislocations are energetically favourable in several cases. In particular, partial twin dislocations which can result in deformation more easily on a $\{1\,1\,0\}$ plane have the lowest line energy. In addition, they showed that stress-aided homogeneous nucleation of twin dislocations is within the reach of thermal energy fluctuations at room temperature, and that the pre-existence of partial twin dislocations may not be necessary for the nucleation of twins.

3.1.2.2. Stress-induced martensitic phase transformation. Occurrence of stress-induced martensitic phase transformations in polymer crystals is indicated by extra reflections in X-ray [188, 223, 230–236] and electron [216, 220, 222] diffraction patterns obtained from deformed single crystals. The presence of such transformations was also detected by i.r. spectroscopy [237]. Tanaka *et al.* [230] found that the martensitic transformations occur as the crystal changes from orthorhombic to monoclinic.

Bevis and Crellin [216] studied also the possible modes of the martensitic transformations in PE and reduced them to four principal modes as illustrated in Fig. 11, based on the magnitudes of the transformation shear strains in each mode. The transformation shear is $\gamma = 0.201$ for modes $T1_1$ and $T1_2$, and $\gamma = 0.318$ for modes $T2_1$ and $T2_2$. Experiments confirmed the existence of martensitic transformations in single crystals [215, 220], in thin melt-crystallized films [52, 223, 229], in bulk material [238], and in oriented specimens [221, 224, 230]. However, the exact modes observed are identified to be $T1_1$ and $T2_1$ in single crystals, and only $T1_1$ in thin melt-crystallized films.

The monoclinic form in PE may be a metastable phase and present only under stress. This was concluded by Kiho *et al.* [239] from the observation that

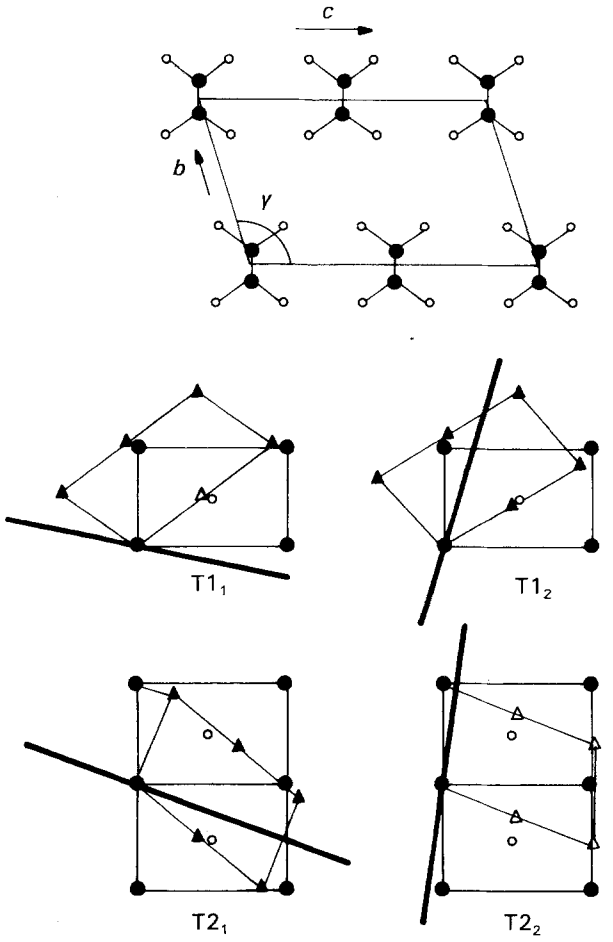

Figure 11 Schematic representation of a monoclinic cell of polyethylene projected on {0 0 1} plane ($a = 0.809$ nm, $b = 0.479$ nm, $c = 0.254$ nm, $\gamma = 107.9°$ [230]) and four most possible modes of martensitic transformation [216].

when deformed single crystals were allowed to relax fully, the monoclinic reflections disappeared. Furthermore, they showed that the monoclinic phase is unstable above 110 °C [240]. However, such reversals of martensitic shear are also possible if the monoclinic portions are surrounded by elastic back-stresses that are not relieved by secondary modes of plastic accommodation, reversing the transformation when the applied stress is removed. Kikuchi and Krimm [53] found that when deformed single crystals were annealed and converted from the monoclinic phase back to the ordinary orthorhombic structure, the crystals changed the fold plane from {1 1 0} to {1 0 0}. This led them to suggest that the monoclinic structure is an intermediate state in the fold-plane transformation.

Stress-induced martensitic transformations occurred before slip was activated in solution-grown single crystals of PE [215]. But in thin melt-crystallized spherulitic film, Allan and Bevis [52] reported that there was no phase transformation until the crystals in spherulites had first undergone twinning and slip as well. Detailed examinations of single-textured PE in compression [221] and tension [192], however, indicate that the CRSS for the martensitic transformation is likely to be of the same order of magnitude as that for chain slip, although the contribution of the martensitic transformation to the total strain is negligible at low stress levels. Clearly, in spherulitic morphology where compatibility between deforming parts needs to be maintained, many of the complementary deformation systems must co-exist.

3.1.3. Deformation of amorphous layers

As discussed in Section 2.2, the commonly accepted model for bulk semi-crystalline polymers consists of lamellar crystals separated from each other by amorphous layers and held together by tie molecules, although the nature of the fold surface and the exact density of tie molecules between lamellae is still not completely understood. Corresponding to this particular morphology, three modes of deformation in the amorphous component have been postulated as being associated with lamellar deformations, which provide additional important degrees of freedom in deformation.

3.1.3.1. Interlamellar shear. This deformation mode involves simple shear of the amorphous region between lamellar crystals with the shear direction being parallel to the lamellae (Fig. 12a). Evidence of interlamellar shear is provided by the variation of lamellar orientation detected by SAXS, in deformed PE both at and above room temperature [178–180, 188, 241–244]. Keller and Pope [179] showed that above 80 °C, interlamellar shear is the dominant mode of deformation of oriented low-density PE (LDPE) in the early phase of deformation. This deformation mode should be a relatively easy mechanism to operate, compared with other modes, above T_g of the amorphous phase which is expected to behave in a rubbery manner with relatively low resistance [149].

The effect of interlamellar shear was well illustrated by Pope and Keller [178], using single-texture LDPE which combines well-developed lamellae, obtained by drawing followed by high-temperature annealing, with a lamellar orientation favourable for interlamellar shear. They showed, using small- and wide-angle diffraction, that as molecular chains rotate past the tensile axis the direction of chain slip reverses, leading to an increase of chain tilting in lamellar crystals and a corresponding decrease in long spacing. This indicates that interlamellar shear is in competition with chain slip during a deformation. The lamellar rotation toward the tensile axis, as a consequence of interlamellar shear, and the chain rotation toward the same tensile axis, as a consequence of chain slip, provide constraints on each other. A similar effect was also observed by Yamada *et al.* [245] in the extension of doubly oriented HDPE.

An almost complete reversibility of interlamellar shear in compression was observed by Young *et al.* [169] and Pope and Keller [178]. The large reversibility in deformation indicates either that the material was rubbery or that the residual stresses of the surrounding undeformed materials were substantial. On the other hand, a certain amount of irreversibility of interlamellar shear in tension was found by Pope and Keller [178]. They suggested that this might be due to breaking of chains of tie molecules, which would

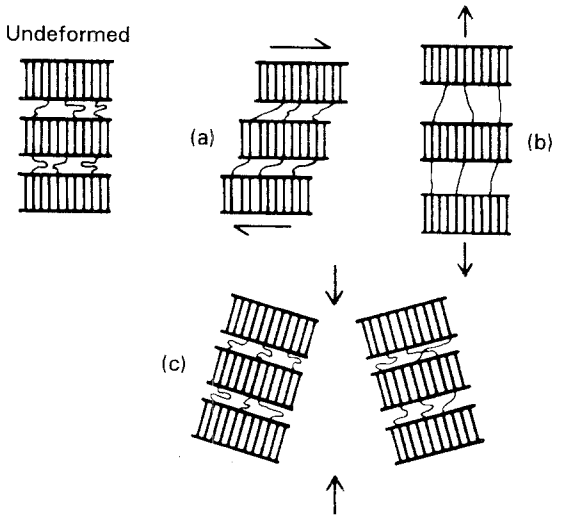

Figure 12 Models of deformation in amorphous regions [149]: (a) interlamellar slip, (b) interlamellar separation, (c) stack rotation.

reduce the residual stresses, or due to the pulling out of chains from lamellae, which would increase the frictional force at lamellar surfaces. Although deformation may occur first in amorphous layers, permanent deformation in the layers requires relatively larger resolved shear stresses. Studies of plastic deformation in textured polymers by several investigators [169, 175, 192] indicated that under normal conditions, the amorphous components of semi-crystalline polymers were "softer" elastically but "tougher" plastically–acting as obstacles to the dislocations in the background crystalline component. Burnay *et al.* [192] estimated that a CRSS of 50 MPa was required to initiate permanent interlamellar slip in their textured samples. This, however, appears excessively high. Recent deformation studies of HDPE by Bartczak *et al.* [2–4] have established that interlamellar shear is dominant in the early phase of deformation at room temperature, and that this deformation is of a rubbery nature. It is nearly fully reversible upon removal of the applied stress.

3.1.3.2. Interlamellar separation. This postulated deformation mode involves changes of the distance between adjacent lamellae (Fig. 12b). As evidence of interlamellar separation, it has been stated that the deformation of crystal lamellae due to chain slip and chain tilting is not able to account for the total change in long-period spacing as indicated by SAXS [178, 179, 246–249], and another mechanism of deformation was necessary. Pope and Keller [178] showed that the amount of interlamellar separation increased with increasing annealing temperature, and attributed this to the fact that annealing at higher temperature resulted in the lamellae being nearly normal to the draw or roll direction, so that there was a high normal stress on the lamellar surfaces. This may be also because a greater amount of low-melting material was rejected by lamellar crystals and formed small imperfect crystals between lamellae during annealing at a higher temperature. The small imperfect crystals were then suspected to deform easily with constant volume and diminish cavitation, thus resulting in ease of interlamellar separation as will be discussed below.

The mechanism of interlamellar separation and hence the resistance to the deformation associated with it must depend upon the detailed structure of the material, including the number and the distribution of active, taut tie molecules between the lamellae and the lateral dimension of the lamellar crystals. In bulk either amorphous matter would have to "flow" into the opening gaps between lamellae from unspecified surroundings, or the mode of interlamellar separation must involve large density changes, i.e. cavitation, in the form of crazing. The former occurred [178, 250] principally in structures composed of one-dimensionally narrow lamellae, which allow the amorphous phase to contract laterally at the edges of the lamellae. The opening gaps can presumably be filled by any extra lamellar material residing between the lamellar stacks or by the parts of lamellae protruding from adjacent stacks [178]. On the other hand, the lateral contraction is constrained in a bulk structure of laterally extended lamellae, and hence interlamellar separation must be accompanied by cavitation between lamellae and becomes more difficult. Flow of amorphous material from the surroundings into the gaps is most unlikely as it would require wholesale rupture of tie molecules. A possible mechanism of accommodating voids between lamellae is by lamellar bending between localized bridges of taut tie molecules, as first suggested by Clark [251]. Such a deformation was found in so-called "elastic hard" material [251–254] which exhibited a high modulus and an extended elastic range. An increase in SAXS intensity accompanying an increase of long-period spacing during deformation of oriented LDPE [179], and large volume changes with whitening of elastic hard samples during deformation [251, 254], have been attributed to cavitation of the samples.

The lateral contraction of interlamellar layers is an explanation, given by Pope and Keller [178], for either the fact that there was no change in the density of the interlamellar layers of samples annealed under 80 °C, as indicated by a very small change in the intensity of the SAXS pattern during stretching, or the fact that for samples annealed at relatively high temperature the strain due to volume increase during stretching was considerably less than the strain of the interlamellar layers. Other possible explanations of the above facts are that small imperfect crystals may be arranged in the interlamellar layers, primarily parallel with the stacks of lamellae, which could deform at constant volume, and that molecular chains may pull out from lamellar crystals and become part of the amorphous layers. The last explanation was shown to be a possibility for PE, since the maximum force suffered by a PE chain before it pulls out from the crystal is less than that necessary for chain breaking [153]. This situation was found to be reversed in nylon [133]. Pope and Keller [178], however, eliminated this as a possible mode in deforming single-texture LDPE, on the argument that interlamellar separation of their samples was largely reversible.

On the macroscopic scale, reversibility of deformation associated with interlamellar separation was found [249] for strains as high as 0.4. The high reversibility of deformations due to interlamellar separation is said to be governed by the rubbery behaviour of the tie molecules between lamellar crystals and the internal residual stresses resulting from the block-like relative displacements of the crystal lamellae. On the other hand, irreversible interlamellar separation was also observed [178, 192]. Burnay *et al.* [192] determined that the stress component normal to the lamellae required to initiate permanent interlamellar separation for their textured samples was approximately 60 MPa.

Clearly, the so-called interlamellar separation reports fall into two categories. Those associated with whitening, or cavitation in bulk or interlamellar rupture in thin films; and those associated with an increase in the long period under stress in highly oriented samples. Since the first process is entirely absent in the deformation in a compression flow achieving the same final texture, it must be recognized as an artefact of tensile deformation. The second possibility can occur also in compression flow, but there is no reliable report of it under these conditions. If it was found to be present in compression flow, it could be entirely due to the stress-induced increase in crystallinity that can in principle be accomplished by the mobility of chain defects that make up the amorphous component in the highly textured materials.

3.1.3.3. Lamella-stack rotation. In order to take up any distortion caused by deformation, particularly in the surrounding amorphous regions, it is often necessary for a stack of lamellae to rotate in a process akin to flow alignment (Fig. 12c). This particular phenomenon was first noted by Groves and Hirsch [255] and was suggested to provide a better explanation of the X-ray data obtained by Cowking *et al.* [241]. By small-angle X-ray scattering in combination with wide-angle X-ray diffraction, Keller and Pope [179] could distinguish, in oriented LDPE, lamellar rotation accompanying deformations including interlamellar shear, interlamellar separation and intralamellar chain slip. A direct observation of rotation of stacks of lamellae was obtained by Tagawa [256] from high-resolution scanning electron micrographs. He reported that the piles of lamellar units containing three to ten lamellar crystals acted as one body and did not separate into single lamellae during deformation.

Rotation of crystalline blocks that are translating over each other due to shearing of material between them is geometrically necessary in the overall kinematics of deformation. It cannot constitute an independent mechanism – not withstanding the obvious additional difficulty that pure rotations of volume elements inside a solid do not produce strain.

In contrast to grain boundary sliding in metal polycrystals, deformation modes in the amorphous regions of polymers offer lower resistance than that offered by the crystalline deformation modes. Peterson and Lindenmeyer [257] showed that the interlamellar shear resistance along the *a* axis is only 2 % of that of intralamellar shear, while the shear along the *b* axis offers a resistance of only 10 % of intralamellar shear. The recent experiments of Bartczak *et al.* [2–4] are in support of this observation. Allan and Bevis [52] studied the deformation processes in thin spherulitic film, and suggested that primary deformation in spherulites is probably due to the interlamellar mechanisms in the early stages of deformation. It seems that lamellar crystals of polymers have fewer slip systems but have softer surroundings than metals. Easier deformations in the amorphous layers provide the possibility of allowing the lamellar crystals to adjust themselves to do better "load sharing".

3.2. Deformation of spherulites

Spherulites, as described earlier, are composed of radially stacked lamellae and interlamellar amorphous regions. The aggregation of space-filling spherulites forms bulk polymers. Therefore, how spherulites behave under applied stresses is one of the most important considerations in understanding the plastic deformation of semi-crystalline polymers, and in linking the macroscopic properties to microscopic structure and deformation modes. The analysis of deformation at the spherulite level is very complex because of the complicated micro-composite morphology of the spherulites. The main difficulties come from the spatial distribution of crystal orientations from point to point, lack of full knowledge of the nature of fold surfaces of lamellae and fold planes of molecules in spherulites, the extent and specific constitution of the amorphous phase between lamellar crystals, and a lack of full understanding of the behaviour of the amorphous material, the properties of which can change significantly as a result of a different crystallization rate.

Experimental investigations on the deformation of spherulites have been carried out by means of light microscopy, X-ray diffraction and electron microscopy on deformed thin films. The deformation processes in crystallites, in amorphous layers, and between spherulites were reported to involve all the deformation mechanisms discussed in the previous section. The nature of the deformation was known to be non-uniform due to the radial orientation of plastically anisotropic lamellar crystals and the presence and extent of amorphous layers. Hay and Keller [177] classified the deformation of spherulites into homogeneous and inhomogeneous types for simplicity, and noted that most of their observations were intermediate between the two types.

In the case of homogeneous deformation, all parts of a spherulite extend simultaneously, and the spherulite is transformed into an ellipsoid in an affine manner (Fig. 13b). Under polarized light, the original concentric and periodic bands of extinction remain in the deformed shape, and the Maltese cross isoclinic lines along the draw direction exhibit a zigzag. The homogeneous deformation was reported [177] to be nearly fully recoverable by either spontaneous retraction or

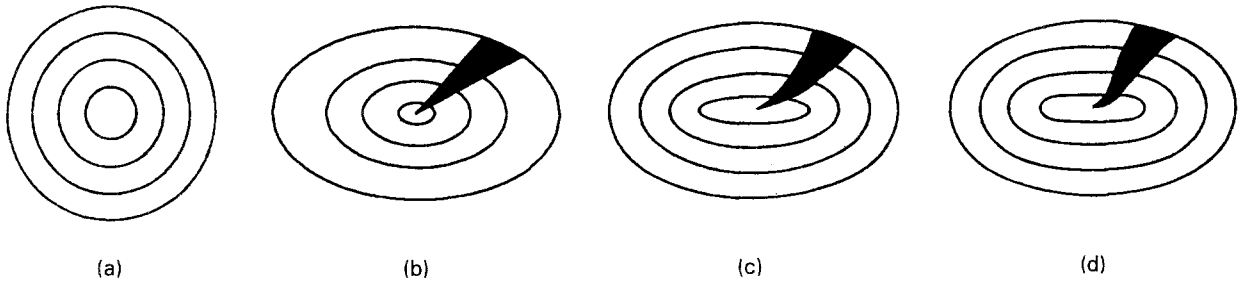

Figure 13 Schematic illustration of homogeneous and inhomogeneous deformation [177]: (a) undeformed spherulite, (b) homogeneously deformed spherulite, (c) inhomogeneously deformed spherulite with radial deforming boundaries, (d) inhomogeneously deformed spherulite with deforming boundary perpendicular to the draw direction.

upon a temperature rise. This elastic behaviour has been interpreted by mechanisms of interlamellar deformation and block-like relative displacements of highly deformed crystalline lamellae.

In homogeneous deformation, yielding and then drawing occurs preferentially in the equatorial regions (Fig. 13c and d), or in regions near the spherulite boundaries, while the remaining parts are undeformed. Further stretching results from the spreading of the drawn regions at the expense of the undeformed regions. The periodic bands of extinction remain in undeformed regions and disappear in the drawn regions. However, on closer inspection under polarized light, changes in the apparently undrawn regions were also noticed, where the dark crosses parallel to the tensile direction become zigzagged. Two types of separation between drawn and undrawn regions were proposed by Hay and Keller [177] as illustrated in Fig. 13c for radial boundaries and in Fig. 13d for boundaries perpendicular to the draw direction.

The recoverable fraction of inhomogeneous deformation is limited. Localization of deformation requires a reduction of plastic resistance which comes about with plastic straining. The inhomogeneous deformation involves both interlamellar and intralamellar mechanisms. Because of the strong dependence of the deformation on lamellar orientation, deformation of spherulites was studied [42, 52, 177, 229, 242, 258–260] in more detail separately in three regions of the spherulite: equatorial, polar, and inclined. There is, however, no clear-cut delineation of the boundaries between these regions.

In the equatorial regions, lamellae are nearly perpendicular to the tensile direction. It was found that the deformation in spherulites occurs in these regions first [42, 177, 260]. Weynant *et al.* [261] observed that the deformation of polybutene-1 begins at the centre of the spherulites and propagates in the equatorial regions along the radial directions. Their observations conform to the theoretical analysis of Wang [262], who predicted a very high stress and strain concentration at the centres of the spherulites. In addition, Wang [262] and Dryden *et al.* [263] predicted stress and strain concentrations around the circumference in the equatorial regions of the spherulites.

According to Hay and Keller [177], the features involved in the deformation in the equatorial regions of spherulites of thin-film PE are interlamellar separation and crystal rotation about the *b* axis, i.e. by (1 0 0) [0 0 1] chain slip. Allan and Bevis [52, 229] carried out a detailed study of deformation processes in PE lamellar crystals in spherulites, and showed that deformation in the equatorial regions involves crystallographic slip in (1 1 0) planes, {1 1 0} mechanical twinning, and stress-induced martensitic transformation of the type $T1_1$. Slip in the [0 0 1] and [1 $\bar{1}$ 0] direction on the (1 1 0) plane is usually favoured in the majority of lamellae. Deformation mechanisms such as interlamellar separation, chain slip and twinning are relatively easier to activate in these regions of the thin films for geometrical reasons relating to the orientation of lamellae.

In the polar regions of the spherulites the chain axes of molecules are always perpendicular to the tensile direction, regardless of the local state of lamellar twist, making the resolved shear stress for chain slip negligible. Hay and Keller [177] suggested that, for alignment of the chain axes parallel to the draw direction, the crystals in the regions should either rotate around the *a* axis as a whole due to some inhomogeneous deformation, or deform by (0 1 0) [0 0 1] chain slip. However, the detailed study by Allan and Bevis [52] indicated that chain slip is not a favoured mode in the polar regions, and that the major deformation mechanisms were (1 1 0) [1 $\bar{1}$ 0] transverse slip and "micro-necking" initiated by slip on the (1 1 0) planes. This must, of course, be associated with local cavitation that permits the very inhomogeneous deformation. Consequently, the polar regions possess a far greater deformation resistance than other regions, which results in the inhomogeneity of spherulite deformation, where local stress concentrations are invariably developed in the polar regions which act as plastic inhomogeneities when the equatorial regions begin to deform.

The deformation behaviour in the inclined regions represents a transition between the two extreme regions around the equators and poles. Allan and Bevis [52] investigated the deformation mechanisms in these regions by selected-area electron diffraction and transmission electron microscopy. Chain slip and slip on the (1 1 0) planes were identified as the predominant modes of deformation in these inclined regions. In addition, their results suggest the occurrence of the {3 1 0} type of mechanical twinning and martensitic transformations, which follow the twinning inside the {3 1 0} twinned crystals. While this is interesting, quite clearly the amount of material involved was small and

the contribution to the overall deformation was probably not large.

The mechanisms of large-strain deformation of initially spherulitic polymers and their consequences have been of intense interest ever since the pioneering experiments of Peterlin [152], who discussed the eventual restructuring of the crystalline lamellae into a new long period. Until recently it had been accepted that a finely dispersed precursor cavitation process was essential for the restructuring of the crystalline layers normal to the principal direction of extension. A version of this process was studied by Galeski *et al.* [264] in nylon 6 deformed in tension. These authors have provided a microstructural processing scenario for how such finely dispersed cavitation can occur in inhomogeneously deforming spherulites. A more universally applicable scenario for reconstruction of the lamellae in spherulites into parallel crystallite blocks perpendicular to the principal extension direction was proposed by Galeski *et al.* [1], based on detailed analysis of incremental deformations during plane-strain compression flow in a channel die where cavitation is completely suppressed. Their model (shown in Fig. 14) indicates that as the lamellae shear, elongate and thin down in the early phase of plastic deformation (Fig. 14a–c), the interface stretching resistance becomes comparable to the plastic resistance of the crystallites (Fig. 14d, at compression ratio near 3.13). After this, the lamellae extensively pinch off by local shear and the released interfaces of the newly created

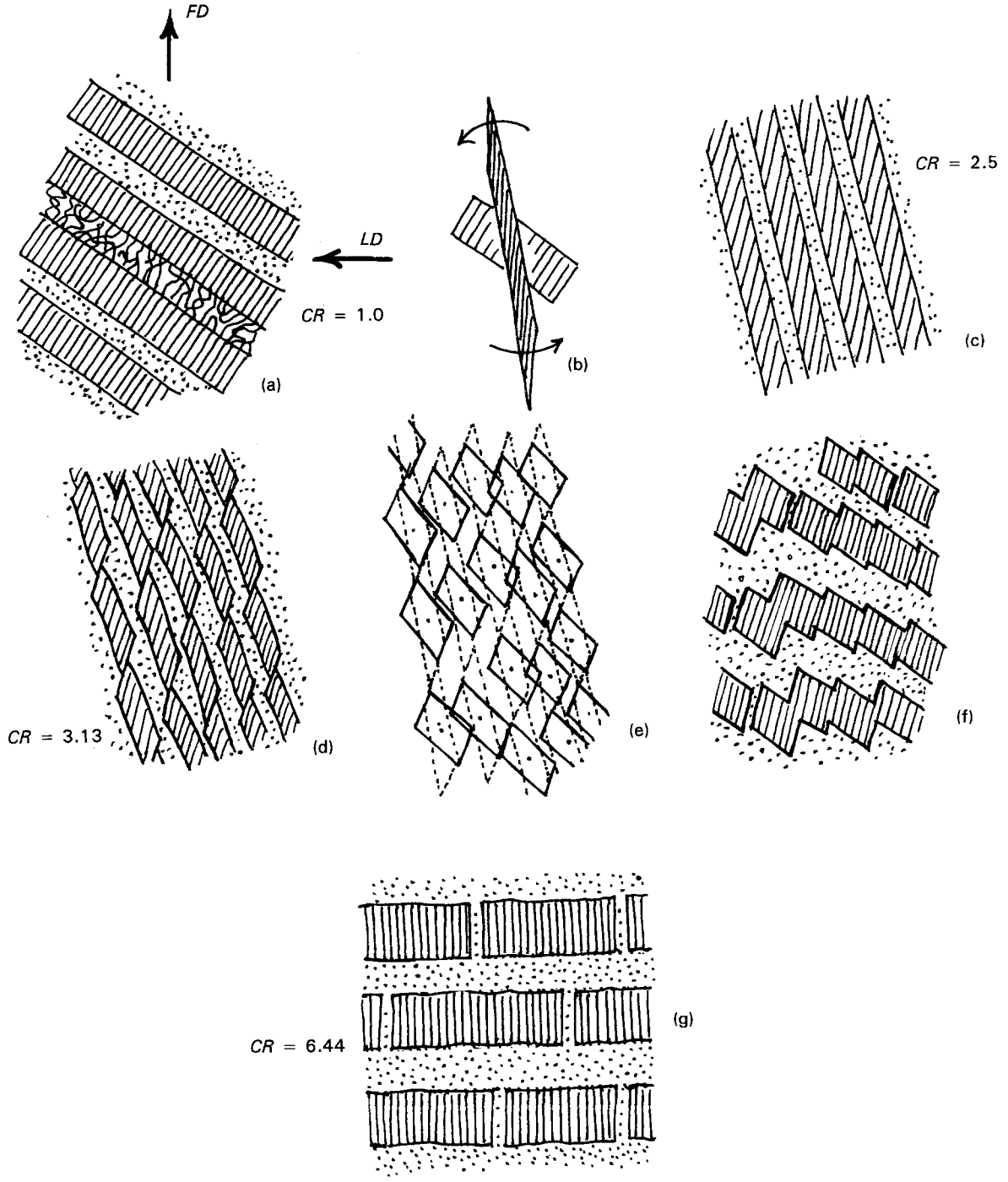

Figure 14 Sketch of the process of the formation of a "new" long period due to a plane strain compression [1]; CR = compression ratio.

crystalline blocks rotate (Fig. 14e and f) to reduce their interface energy – giving rise to the newly reconstructed long period (Fig. 14g).

The deformation in spherulites is highly temperature-dependent [242, 243, 265, 266]. Predecki and Thornton [243] observed pronounced inhomogeneous deformation at the spherulite boundaries at – 20°C. However, at 70°C they found that the deformation within spherulites became almost entirely homogeneous, as might be expected with decreasing overall deformation resistance. With increasing temperature, Oda *et al.* [265] found that the crystal rotation around the *a* axis due to interlamellar shear in the {0 0 1} planes was promoted, while the crystal rotation around the *b* axis due to strain-induced untwisting of lamellae was depressed.

An affine deformation model (Fig. 15b) was first proposed by Wilchinsky [267], who considered the lamellar crystal nature in spherulites and attempted to account for the reorientation of crystals in terms of the affine deformation of spherulites. In the affine deformation model, an undeformed spherical shell (Fig. 15a) inside a spherulite will be transformed into ellipsoidal shells (Fig. 15b), of which the wall thicknesses are not uniform, but proportional to the distance from the centre of the shells. The uniform deformation requires a considerable flow of material within a shell, and thus a considerable expenditure of energy. This situation is aggravated progressively from the inner to the outer shells, which is clearly unrealistic. Measurements of the shape changes of deformed spherulites by Yang and Stein [268] indicated that the affine model is only a first approximation of the actual deformation in spherulites, and that the model is restricted to small strain. In addition, experiments by Hay and Keller [177] showed that the actual ring structure of a spherulite was not in agreement with the deformation pattern of the affine model (Fig. 15b), even in homogeneously deformed spherulites. Kobayashi and Nagasawa [242] found that the mode of deformation in any specific spherulite differs from position to position, and hence it is not possible to describe the deformation with an affine model in any case.

A non-affine model was also proposed by Wilchinsky [267]. The deformation pattern (Fig. 15c) of this model was shown [177] to be in accordance with observations of the ring structure in homogeneously deformed spherulites. The non-affine model assumes that a spherical shell will be deformed into an ellipsoidal shell of approximately uniform thickness, where the strain is assumed to be equalized within a shell. Therefore, such a deformation results in a minimum rearrangement of material, but literally amounts to a pure bending of shells. The displacements of the crystals relative to each other are smaller in the outer shells, and greater in the more highly deformed cores of the spherulites. As a result of the deformation, the structure of an inclined radial region (Fig. 15a) will be transformed into a distorted and contoured region (Fig. 15c) instead of another straight sector (Fig. 15b). This model has difficulty accounting for changes in crystal orientations [205, 259, 269–275].

The most interesting model was the one developed by Wang [262] based on linear elasticity theory. The material element in the model is a composite of radially aligned lamellae and interlamellar amorphous layers which are assumed to be spherically isotropic, i.e. locally isotropic in any plane normal to the radius of the spherulite. The results based on this model gave the local elastic response of spherulites, which was related to optically measured properties by Matsuo *et al.* [276] for small-strain response.

Fig. 16 shows Wang's calculation for a PE sample with 70% crystallinity and subjected to a distant tensile stress σ_z and strain ε_z. It can be seen that all stresses and strains in Fig. 16 vary widely in the spherulite with respect to the crystal orientation relative to the tensile axis. In particular, the stresses and strains tend to infinity at the core of the spherulite. This anomaly is apparently due to the assumption of spherical isotropy, which becomes inadequate at the core region. Nevertheless, the results do show high

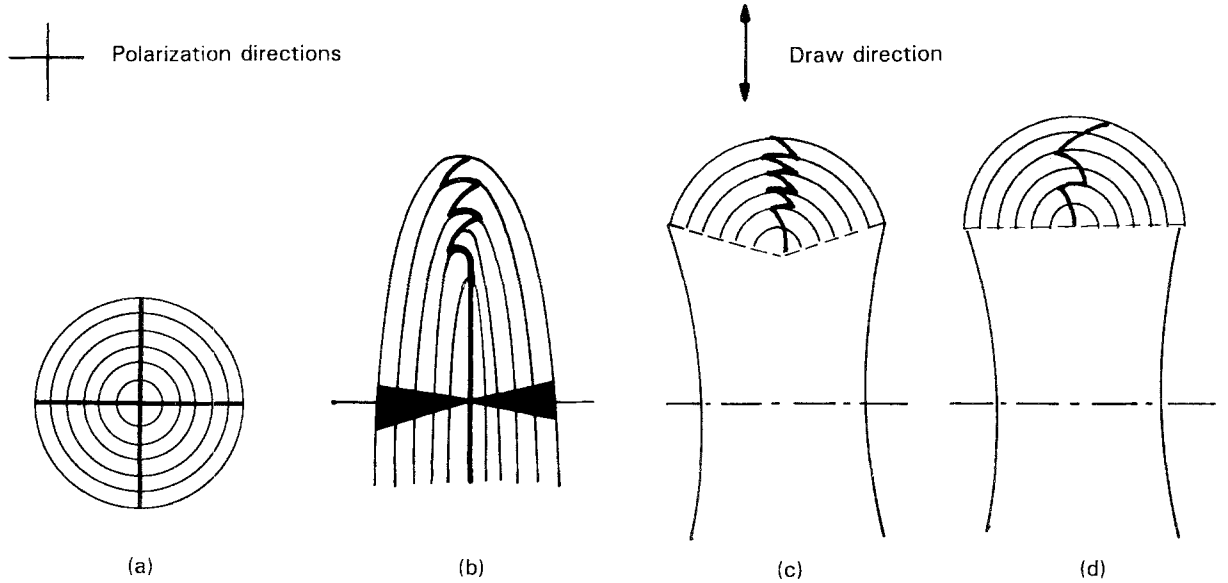

Figure 15 Deformation modes of a spherulite: (a) undeformed state, (b) deformed state based on Wilchinsky's affine model [267], (c) deformed state based on Wilchinsky's non-affine model [267], (d) deformed state based on Wang's non-affine model [262].

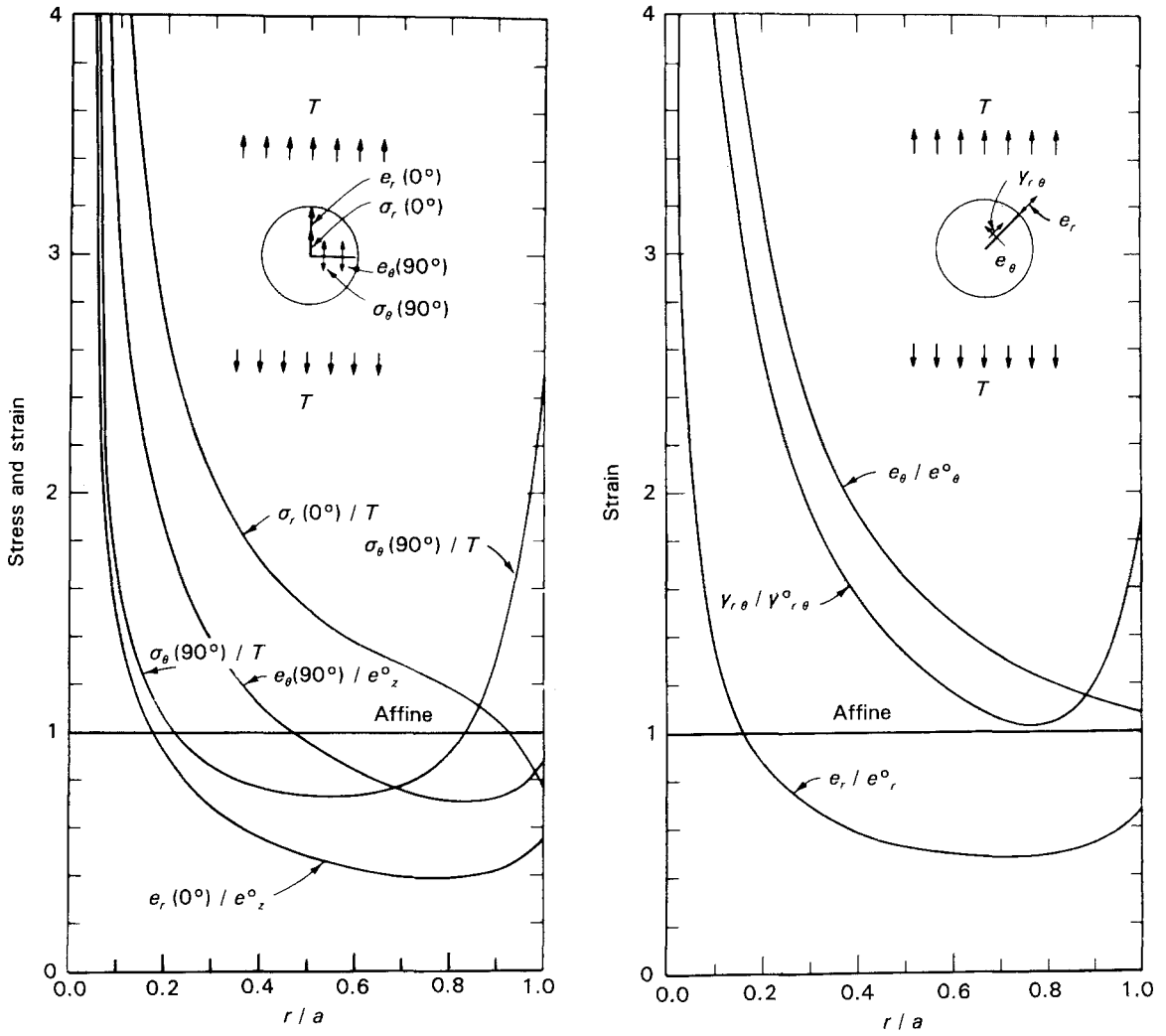

Figure 16 Stresses and strains in a deformed spherulite [262]: (a) in radial elements parallel and normal to the polar (or tensile) axis, (b) in a radial element at 45° from the polar axis.

stress and strain concentration at the centre of the spherulite, which is consistent with actual experimental observations by Keith and Padden [42] and Weynant *et al.* [261]. Note that an affine deformation would result in uniform properties throughout the spherulite, and that the horizontal straight lines in Fig. 16 are corresponding to this situation.

Wang [262] compared his non-affine model with that of Wilchinsky [267] in terms of dimensional changes, and found that the two models agreed reasonably well with a few exceptions. For example, there is little variation in the thickness from shell to shell for the two models (Fig. 15c and d). However, Wang's model predicts an S-shaped distortion for an inclined radial sector. The bends in the lamellae mostly develop near the core and circumference of the spherulite. Consequently, the radial sector tends to elongate appreciably more in Wang's model than in Wilchinsky's single-bend model.

Models similar to Wang's were also proposed by Dryden *et al.* [263] for a singular perturbation analysis, and Matsuo [277] for a linear isothermal viscoelasticity analysis. The analyses of deformation within spherulites by Wang [262], Dryden *et al.* [263] and Matsuo [277] are appropriate for relating the local response of the spherulites to the deformation of the bulk material, but are not able to provide information on crystal reorientation. This is because the material element considered in their continuum approaches is assumed to be spherically isotropic to make the problem tractable, and is in fact composed of a large number of small material units such as lamellae and amorphous layers. In order to study dimensional changes of individual crystallites, and further, the evolution of texture of semi-crystalline polymers, models must be constructed at progressively finer microscopic levels incorporating the specific morphology of the material. The models need to be able to relate the local deformation of spherulites to those of lamellar crystals and amorphous layers. On the other hand, to follow the whole picture of deformation on the macro-scale, the physically based microstructural theories for polymers must be related to continuum plasticity theories, as was done first by Asaro [278] for metal polycrystals through elastic–plastic models with kinematic-type hardening. Such models have been specifically developed for HDPE morphologies by Parks and Ahzi [12] and in more refined form by Lee *et al.* [14] with intermediate forms developed by Ahzi *et al.* [13] for a composite crystalline lamella and amorphous layer model to predict texture development during large-strain deformation. A comparison of these predicted textures with experiments has been given by Lee *et al.* [15].

3.3. Macroscopic continuum behaviour

Data from macroscopic mechanical experiments contain much information on the intrinsic micromechanical properties of materials, although other knowledge and some imagination are required to distribute them to individual microscopic mechanisms. In relating to microscopic properties, it is the "true" or local macroscopic behaviour that is most important or relevant. It is more complicated to measure or achieve the true values when dealing with polymers deformed in tension because of the early occurrence of necking and subsequent stabilized neck propagation. Using the conventional engineering stress, engineering strain and constant strain rate obtained by a constant velocity of crosshead motion of the testing machine can lead to rather erroneous impressions regarding strain hardening or softening, the rate of hardening, etc.

True stress–strain data were obtained by Meinel and Peterlin [279], who measured the elongation of a very fine grid printed on the specimen by means of a photographic technique, and defined the "true stress" and "true strain" as

$$\sigma = \frac{P}{A} = \frac{P}{A_0}\left(\frac{l}{l_0}\right) \tag{2}$$

and

$$\varepsilon = \lim_{l_0 \to 0} [\ln (l/l_0)] \tag{3}$$

where l_0 and l are mesh lengths of the grid before and after deformation, respectively. Because the grid was small and the strain could be considered to be homogeneous within a single mesh length, the data obtained [279] represented more closely the real local properties of the material, except that the imposed constant strain rate was still an average over the whole specimen, and was based on constant grip velocity.

When specifically considering the strain-rate effect for polymers, G'Sell and Jonas [280] introduced an elegant method by which the true stress versus true strain curve can be obtained at "true constant strain rate". In their tensile test, they measured continuously the diameter (D) at the neck of a cylindrical specimen by means of a closed-loop tensile machine and calculated the true stress and true strain by

$$\sigma = 4P/\pi D^2 \tag{4}$$

and

$$\varepsilon = 2\ln (D_0/D) \tag{5}$$

where the influence of stress triaxiality was ignored and the material was assumed to be incompressible. A nominally true constant strain rate is then achieved by manipulating the crosshead velocity through a feedback control loop to maintain the rate of change of Equation 5 constant. In the interpretation of their experimental results [281], they gave a very useful insight into the properties of several polymers. The stress–strain curves in Fig. 17 were obtained under nominally true constant strain rate, at least until the diametral reduction rate vanishes when the shoulders move away along the length of the specimen. G'Sell and Jonas showed that the strain-rate sensitivity of polymers is not as high as might be expected (a typical conventional plastic strain-rate sensitivity coefficient being $m = 0.06$ for PE, i.e. of the same order as for metals at room temperature). Thus, the stabilization of flow localization in the neck region of polymers is due to the positive curvature of the true stress–strain curve, as has been remarked by many investigators [282], instead of being due to an increase in local strain rate.

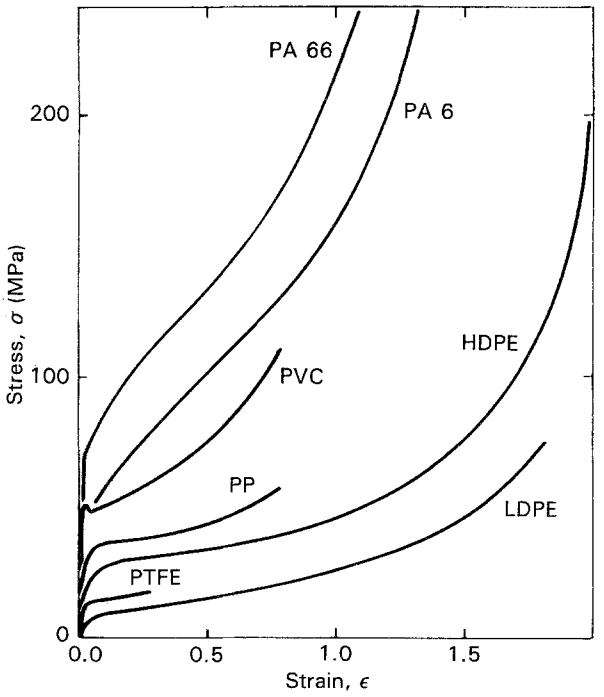

Figure 17 True stress against true strain curves of several polymers [281]; $\dot{\varepsilon} = 10^{-3}\,s^{-1}$.

G'Sell and Jonas [281] also performed rapid strain-rate change experiments, which are used widely to determine rate sensitivity in metals. Fig. 18 shows their results. According to G'Sell and Jonas, the memory of the previous strain rate is retained only during the transient period, while the behaviour after the transient seems to be independent of the earlier plastic strain history and depends only on the current strain and strain rate. Two extremes of the transients are the "normal" transient and the "inverse" transient, which are characterized by a rounded shape of stress–strain curve and a marked overshoot of true stress, respectively. In addition, G'Sell and Jonas [281] performed transient tests involving stress relaxation at fixed diameter followed by resumption of straining at a constant reference strain rate, and abrupt loading of the samples for various intervals followed by resumption of straining.

Shinozaki and his coworkers [283–290] studied various types of stress–strain curves of PE and polypropylene in detail, and attempted to relate their results using the methods of continuum mechanics to microstructural mechanisms of deformation based on the theoretical models developed by Asaro [278] for metals. Although the curve they examined and the strain rate applied were not defined as carefully as by G'Sell and Jonas [281], an insight into the mechanical

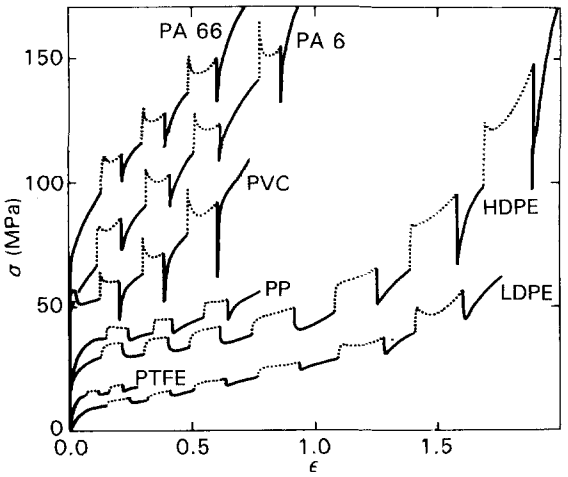

Figure 18 Transient behaviour of strain-rate changes of several polymers [281]: (——) $\dot{\varepsilon} = 10^{-3}\,s^{-1}$, (···) $\dot{\varepsilon} = 10^{-2}\,s^{-1}$.

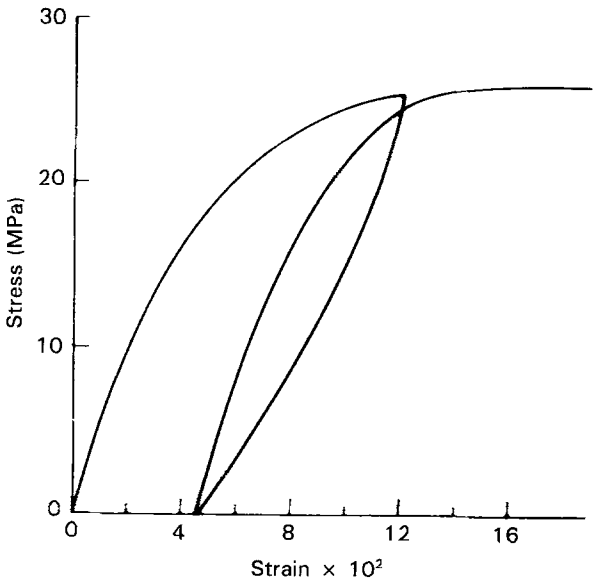

Figure 19 Stress against strain curves with loading, unloading and reloading in tension [283].

behaviour of polymers can be obtained from their studies, particularly from their pre-necking and cyclic deformation results.

By carefully examining one of their stress–strain diagrams (Fig. 19), it can be seen that both initial loading and reloading curves even before gross yielding do not show exactly a linear behaviour, and that the reloading curve before gross yielding is not closely parallel to the original loading curve. The non-linear behaviour before gross yielding may be due to microscopic inhomogeneity of deformation. For instance, stress concentrations around the centres and circumferences in equatorial regions of spherulites may cause plastic flow in these regions at early stages of deformation before overall yielding is reached, which can result in the non-linear behaviour of the initial loading curve. The early occurrence of inhomogeneous plastic deformation changes the microstructure of the material, which results in the diversion of the reloading curve from the original one.

Experimentally, the total plastic deformation resistance of semi-crystalline polymers at any strain could be partitioned into two components by means of stress-relaxation dip tests proposed by Li *et al.* [291] and modified by Lloyd and Embury [292] and Solomon *et al.* [293]. These two parts of the total resistance to deformation can be considered as a first approximation as a strain-dependent portion and a rate-dependent portion, as

$$\sigma = \sigma_0(p, T, \dot{\varepsilon}) + \sigma'(\varepsilon) \qquad (6)$$

which is similar to the partition of the flow stress noted for glassy polymers [294]. The first term (σ_0) on the right-hand side of the equation is called the effective stress, which may depend on hydrostatic pressure (p), temperature (T) and strain rate ($\dot{\varepsilon}$). The second term (σ') is the internal stress (or back stress) which is nearly dependent on the strain alone.

The internal stress or back stress is the driving force for recovery of plastic deformation. It is associated with the overall increase of free energy stored in the deformed polymer. The exact origin(s) or contribution(s) of the internal stress has not always been fully understood in a semi-crystalline polymer, although a number of possibilities have been suggested by several investigators. Inhomogeneity of local plastic deformation, which is most likely to be the case in polymers because of the lamellar composition of the spherulitic morphology, is clearly a very important cause in the development of internal stress [283]. This particular part of the internal stress may be called transformation-induced back stress, and is associated with the increase of internal strain energy due to inhomogeneous shear transformations in the polymer. Changes in configurational entropy due to deformation, most likely in the amorphous phase as observed by a number of investigators [294–296], must play an important role in the total internal stress. This particular component may be called entropy-induced back stress. Peterson [297] and Pope and Keller [178] suggested another driving force which may result in the recovery of plastic deformation. This driving force for recovery is associated at least in part with an increase in internal energy due to an increase in surface free energy during crystallite deformation by chain tilting. The various parts of the internal stress can only be differentiated on the basis of specific microscopic models, while the other internal stress is measured by macroscopic experiments.

Work-hardening behaviour and associated Bauschinger effect of polymers are directly related to the internal stress. Chaki and Li [298] designed an experiment to examine these properties of LDPE in detail. They found the existence of latent hardening in one direction and softening (Bauschinger effect) in another after the specimen was compressed in the third direction. They suggested that a certain orientation distribution of plastic strain produced by the primary deformation created a molecular orientation arrangement which would result in hardening or softening in other directions. This concept was developed further and more precisely by Boyce *et al.* [296] for glassy polymers on a configurational entropy model used in rubber elasticity, and generalized further for multiaxial deformation by Arruda and Boyce [299]. These

developments for glassy polymers have been effectively incorporated by Lee *et al.* [14] into a general large-strain semi-crystalline polymer deformation computer code to represent the behaviour of the amorphous component of the material.

The macro-behaviour of pressure dependence [300] and temperature dependence [301] of plastic deformation of PE were studied by Davis and Pampillo. Fig. 20 shows the relation between tensile yield stress and pressure. It is in accord with the micro-yield criterion (Equation 1) proposed by Keller and Rider [166]. Davis and Pampillo pointed out that in relation to their experimental results the pressure activation volume, $kT(\partial \ln \dot{\varepsilon}/\partial p)_{T,\varepsilon}$, is an appropriate parameter that characterizes the pressure dependence of plastic deformation of PE.

Fig. 21 shows the temperature dependence of the flow stress for homogeneous flow at four different homogeneous strains. Pampillo and Davis [301] found that at approximately 175 and 265 K there were changes in the slopes of the stress–temperature curves.

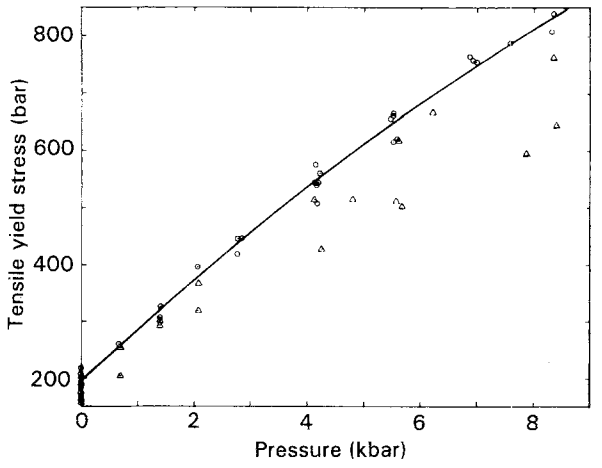

Figure 20 Tensile yield stress as a function of pressure [300]; 1 bar $= 10^5$ Pa.

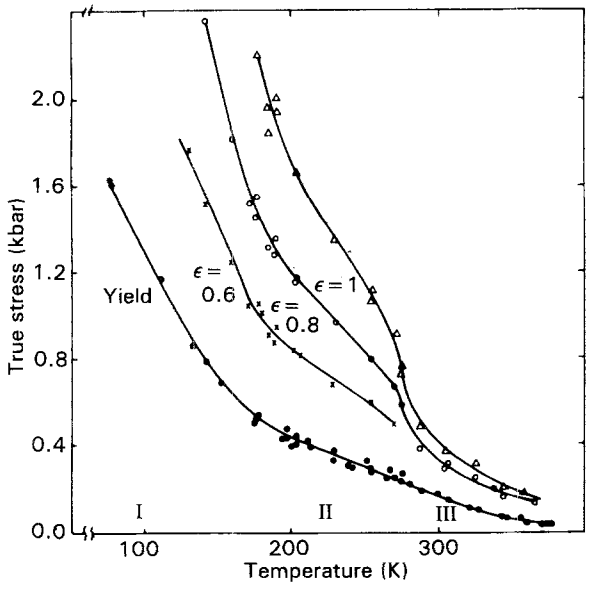

Figure 21 Tensile yield stress as a function of temperature [301]; 1 bar $= 10^5$ Pa. (●) Yield, (×) $\varepsilon = 0.6$, (○) $\varepsilon = 0.8$, (△) $\varepsilon = 1.0$.

They attempted to relate the changes of the slopes to transitions between rate-controlling mechanisms of deformation.

4. Discussion

Semi-crystalline polymeric solids are heterogeneous media in which understanding the large-strain plastic deformation behaviour in more than a qualitative sense requires some understanding of the structure of both the amorphous and the lamellar crystalline components and their deformation mechanisms. Because of the simplicity of its molecular architecture and its crystal structure, HDPE is the semi-crystalline polymer of choice for mechanistic studies. In spite of the large number of detailed studies which we have reviewed above, a certain controversy still exists on the nature of the division between the amorphous and the crystalline components of HDPE, and the nature of the interface between the two. The available evidence for the melt-crystallized material is that the crystalline lamellae are more a result of "chain association" rather than "chain folding" and that the intervening amorphous layers are best viewed as phase-separated chain packing defects of the crystalline components, where molecules of one lamella weave as often into the neighbouring crystallite as folding back into the one from which they emerged. This has important consequences for the large-strain plastic flow behaviour through the degree of mechanical coupling of the two components. The relatively high density of the so-called tie-links that stitch the lamellae together result in an early soft behaviour of the amorphous component between lamellae but a relatively quick "locking" behaviour later, which then throws the action from the amorphous to the crystalline component. It is for this reason that after the initial soft behaviour is taken up at strain levels of the order of 0.25 the subsequent deformation is very well characterized by the deformation of the crystalline component alone. This manifests itself also in a saturation of the potentially recoverable strain component in the amorphous material upon unloading at about this strain level. As might be expected, this recovery strain resulting from the early inhomogeneous deformation concentrated in the amorphous component will saturate once this component "locks up", requiring the crystalline component to also deform and leading to more homogeneous overall plastic deformation with a relatively stationary level of internal stresses.

Experiments in plane-strain compression of HDPE [1], and associated computer simulations [14, 15] treating the material as a combination of a polycrystalline aggregates and intervening amorphous layers, show that for compressive equivalent strains up to about 1.2 the material deforms compatibly, with the crystalline–amorphous interfaces remaining distinct in space and undergoing no significant lateral translation. In this range the computer simulation predicts very successfully the evolution of both crystallographic deformation textures and morphological textures of lamellar orientation [15]. The experiments demonstrate that around this strain the stretched-out

crystalline lamellae undergo extensive fragmentation by apparent local slip-induced pinch-off followed by extensive lateral translation of the crystalline–amorphous interfaces, giving a progressive reconstruction of the amorphous component into layers roughly normal to the principal molecular orientation in the crystalline component as described in detail by Galeski *et al.* [1]. In addition, deconvolution of the wide-angle X-ray scattering information [1] indicates that beyond this stage the molecular alignment in the amorphous component becomes nearly as complete as in the crystalline component and acquires a diffuse but well recognizable hexagonal symmetry. This indicates that for deformations exceeding this strain, a long-range coherence of aligned molecules is discernible over many characteristic dimensions of the thicknesses of lamellae, as the intensity of the SAXS information from the reconstructed amorphous layers progressively decreases. At strains of the order of 1.85 the deformation texture obtained in plane-strain compression closely resembles that of an orthorhombic single crystal of HDPE. In nylon 6 [8] and PET [10] with monoclinic and triclinic crystal structures the result is an anisotropic structure having orthotropic symmetry with a well divided bimodal aggregation of the oriented crystallites. The observed extensive interface translation accompanying the pinching-off of lamellae reinforces the view that the amorphous component consisting of the tie-links should not be viewed as a distinct material, but as an aggregation of chain defects of the crystalline component that have potential mobility along the chains. For equivalent strains exceeding 1.85 in plane-strain deformation the previously established quasi-single crystalline texture is gradually replaced by a fibre texture by the time the strains have reached a level of the order 2.50. A similar texture development scenario is observed also in simple shear [4], leading first to a quasi-single crystalline texture and then to a nearly fully developed fibre texture, without, however, the corresponding strong restructuring of a long period by lamellar pinch-off that was found in plane-strain compression. While it is clear that the degradation of the quasi-single crystalline texture into a fibre texture is a result of activity by lesser mechanisms of transverse slip on both the (1 0 0) and the (0 1 0) planes, with a trace of twinning mixed in, the kinematical necessity for such deformation is not fully clear. Parenthetically, we note here that in all this described textural alteration in compressive and shear flow, particularly in the restructuring of the long period by lamellar pinch-off, the alterations are accomplished without any observable internal cavitation of the type that has been noted in tension and referred to as "micro-necking". Thus, the previously established notion that such internal cavitation is essential for fully developed texturing must be abandoned. This cavitation is an artefact of the tensile mode of deformation.

While the recent developments summarized above have clarified the kinematics of deformation of the amorphous and the crystalline components, much still needs to be accomplished to fully understand the rate mechanism of plastic flow in both the crystalline and the amorphous components. Moreover, the views emerging from the kinematics of large-strain plastic deformation have important implications in the threading of molecules between the crystalline and amorphous components which, in turn, may require re-examination of the molecular kinematics involved during crystallization.

Acknowledgements

This research has been supported by the Defense Advanced Research Projects Agency through the Office of Naval Research under contract N00014-86-K-0768. We are grateful for discussions with many investigators but notably with A. Galeski, R. E. Cohen, P. H. Geil, S. Krimm, D. M. Parks and A. Ziabicki.

References

1. A. GALESKI, Z. BARTCZAK, A. S. ARGON and R. E. COHEN, *Macromolecules* **25** (1992) 5705.
2. Z. BARTCZAK, A. S. ARGON and R. E. COHEN, *ibid.* **25** (1992) 5036.
3. *Idem, ibid.* **25** (1992) 4692.
4. *Idem, Polymer* in press.
5. H. H. SONG, A. S. ARGON and R. E. COHEN, *Macromolecules* **23** (1990) 870.
6. A. GALESKI, A. S. ARGON and R. E. COHEN, *ibid.* **24** (1991) 3953.
7. *Idem, ibid.* **24** (1991) 3945.
8. L. LIN and A. S. ARGON, *ibid.* **25** (1992) 4011.
9. *Idem, ibid.* in press.
10. A. BELLARE, R. E. COHEN and A. S. ARGON, *Polymer* **34** (1993) 1393.
11. J. RAKESTRAW, R. E. COHEN and A. S. ARGON, to be published.
12. D. M. PARKS and S. AHZI, *J. Mech. Phys. Solids* **38** (1990) 701.
13. S. AHZI, D. M. PARKS and A. S. ARGON, "Computer Modeling and Simulation of Manufacturing Processes" (ASME, New York, 1990) **20**, 287.
14. B. J. LEE, D. M. PARKS and A. S. ARGON, *J. Mech. Phys. Solids*
15. B. M. LEE, A. S. ARGON, D. M. PARKS, S. AHZI and Z. BARTCZAK, *Polymer* **34**, (1993) 3555.
16. Proceedings of Conference on Crystallization of Polymers, Université de Mons-Hainaut, Belgium, September 1992, in press.
17. P. H. GEIL, "Polymer Single Crystals" (Interscience, New York, 1963).
18. A. KELLER, *Rep. Prog. Phys.* **31** (Part II) (1968) 623.
19. F. KHOURY and E. PASSAGLIA, in "Treatise on Solid State Chemistry", Vol 3, edited by N. B. Hannay (Plenum, New York, 1976) p. 335.
20. P. H. TILL Jr, *J. Polym. Sci.* **24** (1957) 301.
21. A. KELLER, *Phil. Mag.* **2** (1957) 1171.
22. E. W. FISCHER, *Z. Naturforsch.* **12A** (1957) 753.
23. A. KELLER and A. O'CONNOR, *Disc. Faraday Soc.* **25** (1958) 114.
24. F. KHOURY and L. H. BOLZ, in "38th Annual Proceedings of the Electron Microscopy Society of America", San Francisco, California, edited by G. W. Baily (Claitors, Baton Rouge, 1980) p. 242.
25. D. H. RENEKER and P. H. GEIL, *J. Appl. Phys.* **31** (1960) 1916.
26. P. H. LINDENMEYER, *J. Polym. Sci. C* **1** (1963) 5.
27. H. GLEITER and J. PETERMANN, *J. Polym. Sci. B* **10** (1972) 877.
28. W. D. NIEGISCH and P. R. SWAN, *J. Appl. Phys.* **31** (1960) 1906.
29. D. C. BASSETT and A. KELLER, *Phil. Mag.* **6** (1961) 345.
30. S. J. ORGAN and A. KELLER, *J. Mater. Sci.* **20** (1985) 1571.
31. T. KAWAI and A. KELLER, *Phil. Mag.* **11** (1965) 1165.

32. H. D. KEITH, *J. Appl. Phys.* **35** (1964) 3115.
33. D. J. BLUNDELL and A. KELLER, *J. Macromol. Sci–Phys.* **B2** (1968) 337.
34. D. C. BASSETT, F. C. FRANK and A. KELLER, *Nature* **184** (1959) 810.
35. *Idem, Phil. Mag.* **8** (1963) 1739.
36. *Idem, ibid.* **8** (1963) 1753.
37. A. KELLER, *Kolloid-Z. Z. Polym.* **197** (1964) 98.
38. H. D. KEITH and F. J. PADDEN Jr, *J. Polym. Sci.* **39** (1959) 101.
39. A. KELLER, *ibid.* **39** (1959) 151.
40. P. H. LINDENMEYER and V. F. HOLLAND, *J. Appl. Phys.* **35** (1964) 55.
41. A. KELLER, *Nature* **169** (1952) 913.
42. H. D. KEITH and F. J. PADDEN Jr, *J. Polym. Sci.* **41** (1959) 525.
43. J. E. BREEDON, J. F. JACKSON, M. J. MARCINKOWSKI, and M. E. TAYLAR Jr, *J. Mater. Sci.* **8** (1973) 1071.
44. P. H. GEIL, *J. Polym. Sci. C* **13** (1966) 149.
45. R. P. PALMER and A. J. COBBOLD, *Makromol. Chem.* **74** (1964) 174.
46. A. KELLER and S. SAWADA, *ibid.* **74** (1964) 190.
47. A. KELLER, *J. Polym. Sci.* **17** (1955) 351.
48. D. C. BASSETT and A. M. HODGE, *Proc. Roy. Soc.* **A377** (1981) 25.
49. D. C. BASSETT, A. M. HODGE and R. H. OLLEY, *ibid.* **A377** (1981) 39.
50. M. I. BANK and S. KRIMM, *J. Polym. Sci. A-2* **7** (1969) 1785.
51. R. J. YOUNG and P. B. BOWDEN, *J. Mater. Sci.* **8** (1973) 1177.
52. P. ALLAN and M. BEVIS, *Phil. Mag.* **41** (1980) 555.
53. Y. KIKUCHI and S. KRIMM, in "Plastic Deformation of Polymers", edited by A. Peterlin (M. Dekker, New York, 1971) p. 7.
54. F. RYBNIKAR, *J. Polym. Sci.* **44** (1960) 517.
55. A. PETERLIN, *J. Appl. Phys.* **35** (1964) 75.
56. J. M. SCHULTZ and R. D. SCOTT, *J. Polym. Sci. A-2* **7** (1969) 659.
57. A. SHARPLES, "Introduction to Polymer Crystallization" (Arnold, London, 1966).
58. T. W. HUSEBY and H. E. BAIR, *J. Appl. Phys.* **39** (1968) 4969.
59. R. G. BROWN and R. K. EBY, *ibid.* **35** (1964) 1156.
60. J. D. HOFFMAN, G. T. DAVIS and J. I. LAURITZEN, in "Treatise on Solid State Chemistry", Vol 3, edited by N. B. Hannay (Plenum, New York, 1976) p. 497.
61. J. D. HOFFMAN and J. J. WEEKS, *J. Chem. Phys.* **42** (1965) 4301.
62. J. MARTINEZ-SALAZAR, P. J. BARHAM and A. KELLER, *J. Mater. Sci.* **20** (1985) 1616.
63. P. J. BARHAM, D. A. JARVIS and A. KELLER, *J. Polym. Sci. A-2* **20** (1982) 1733.
64. S. J. ORGAN and A. KELLER, *J. Mater. Sci.* **20** (1985) 1602.
65. P. J. BARHAM, R. A. CHIVERS, A. KELLER, J. MARTINEZ-SALAZAR and S. J. ORGAN, *ibid.* **20** (1985) 1625.
66. E. W. FISCHER and G. F. SCHMIDT, *Angew. Chem.* **74** (1962) 551.
67. D. C. BASSETT and A. KELLER, *J. Polym. Sci.* **40** (1959) 565.
68. S. J. ORGAN and A. KELLER, *J. Mater. Sci.* **20** (1985) 1586.
69. D. C. BASSETT, A. KELLER and S. MITSUHASHI, *J. Polym. Sci. A* **1** (1963) 763.
70. B. WUNDERLICH and T. ARAKAWA, *ibid.* **2** (1964) 3697.
71. P. H. GEIL, F. R. ANDERSON, B. WUNDERLICH and T. ARAKAWA, *ibid.* **2** (1964) 3703.
72. T. HATAKEYAMA, H. KANETSUNA and T. HASHIMOTO, *J. Macromol. Sci.–Phys.* **B7** (1973) 411.
73. R. H. OLLEY and D. C. BASSETT, *J. Polym. Sci., Polym. Phys. Ed.* **15** (1977) 1011.
74. D. C. BASSETT and B. TURNER, *Phil. Mag.* **29** (1974) 925.
75. *Idem, Nature, Phys. Sci.* **240** (1972) 146.
76. M. YASUNIWA, C. NAKAFUKU and T. TAKEMURA, *Polym. J.* **4** (1973) 526.
77. D. C. BASSETT, S. BLOCK and G. J. PIERMARINI, *J. Appl. Phys.* **45** (1974) 4146.
78. K. TAKAMIZAWA, H. HASEGAWA and Y. URABE, *Polym. Prepr. Jpn* **27** (1978) 493.
79. Y. MAEDA and H. KANETSUNA, *J. Polym. Sci., Polym. Phys. Ed.* **12** (1974) 2551.
80. *Idem, ibid.* **14** (1976) 2057.
81. Y. MAEDA, H. KANETSUNA, K. TAGASHIRA and T. TAKEMURA, *ibid.* **19** (1981) 1313.
82. Y. MAEDA, H. KANETSUNA, K. NAGATA, K. MATSUSHIGE and T. TAKEMURA, *ibid.* **19** (1981) 1325.
83. R. A. FAVA, *J. Polym. Sci. D: Macromol. Rev.* **5** (1971) 1.
84. A. KELLER, *Kolloid-Z. Z. Polym.* **231** (1969) 386.
85. A. PETERLIN, *J. Macromol. Sci.–Phys.* **B3** (1969) 19.
86. P. J. FLORY, *J. Amer. Chem. Soc.* **84** (1962) 2857.
87. E. W. FISCHER and R. LORENZ, *Kolloid-Z. Z. Polym.* **189** (1963) 97.
88. M. STAMM, E. W. FISHER, M. DETTENMAIER and P. CONVERT, *Faraday Disc. Chem. Soc.* **68** (1979) 263.
89. L. MANDELKERN, *Acc. Chem. Res.* **9** (1976) 81.
90. *Idem, J. Polym. Sci. C* **50** (1975) 457.
91. F. C. FRANK and P. J. FLORY, in "Growth and Perfection of Crystals", edited by R. H. Doremus, B. W. Roberts and D. Turnbull (Wiley, New York, 1958) p. 529.
92. F. C. FRANK, *Faraday Disc.* **68** (1979) 7.
93. C. M. GUTTMAN, E. A. DIMARZIO and J. D. HOFFMAN, *Polymer* **22** (1981) 1466.
94. P. H. LINDENMEYER, *J. Polym. Sci. C* **20** (1967) 145.
95. A. KELLER and D. J. PRIEST, *J. Macromol. Sci.–Phys.* **B2** (1968) 479.
96. D. E. WITENHAFER and J. L. KOEING, *J. Polym. Sci. A-2* **7** (1969) 1279.
97. M. I. BANK and S. KRIMM, *J. Appl. Phys.* **40** (1969) 4248.
98. A. J. KOVACS, A. GONTHIER and C. STRAUPE, *J. Polym. Sci. C* **50** (1975) 283.
99. E. N. DALAL and P. J. PHILLIPS, *Macromolecules* **17** (1984) 248.
100. D. C. BASSETT, "Principles of Polymer Morphology" (Cambridge University Press, London, 1981).
101. F. C. FRANK and M. TOSI, *Proc. Roy. Soc.* **A263** (1961) 323.
102. J. I. LAURITZEN Jr and E. PASSAGLIA, *J. Res. Nat. Bur. Stds* **71A** (1967) 261.
103. A. KELLER, E. MARTUSCELLI, D. J. PRIEST and Y. UDAGAWA, *J. Polym. Sci. A-2* **9** (1971) 1807.
104. A. KELLER, in "Macromolecular Science", Vol. 8, edited by C. E. H. Bawn (Butterworths, London, 1972) p. 105.
105. M. TASUMI and S. KRIMM, *J. Polym. Sci. A-2* **6** (1968) 995.
106. M. I. BANK and S. KRIMM, *J. Polym. Sci. B* **8** (1970) 143.
107. S. KRIMM and T. C. CHEAM, *Faraday Disc.* **68** (1979) 244.
108. X. JING and S. KRIMM, *J. Polym. Sci. B* **21** (1983) 123.
109. P. J. FLORY and D. Y. YOON, *Nature* **272** (1978) 226.
110. J. KLEIN and R. BALL, *Faraday Disc.* **68** (1979) 198.
111. E. A. DiMARZIO, C. M. GUTTMAN and J. D. HOFFMAN, *ibid.* **68** (1978) 210.
112. P. G. DeGENNES, *J. Chem. Phys.* **55** (1971) 572.
113. J. SCHELTEN, D. G. H. BALLARD, G. D. WIGNALL, G. LONGMAN and W. SCHMATZ, *Polymer* **17** (1976) 751.
114. J. S. HIGGINS and R. S. STEIN, *J. Appl. Crystallogr.* **11** (1978) 346.
115. R. ULLMAN, *Ann. Rev. Mater. Sci.* **10** (1980) 261.
116. L. H. SPERLING, *Polym. Eng. Sci.* **24** (1984) 1.
117. D. M. SADLER and A. KELLER, *Polymer* **17** (1976) 37.
118. *Idem, Macromolecules* **10** (1977) 1128.
119. *Idem, Science* **203** (1979) 263.
120. D. Y. YOON and P. J. FLORY, *Polymer* **18** (1977) 509.
121. D. Y. YOON, *J. Appl. Crystallogr.* **11** (1978) 531.
122. D. Y. YOON and P. J. FLORY, *Faraday Disc.* **68** (1979) 288.
123. J. SCHELTEN, G. D. WIGNALL and D. G. H. BALLARD, *Polymer* **15** (1974) 682.
124. C. M. GUTTMAN, J. D. HOFFMAN and E. A. DiMARZIO, *Faraday Disc.* **68** (1979) 297 and general discussion remarks of C. M. Guttman, p. 457.
125. H. D. KEITH, F. J. PADDEN Jr and R. G. VADIMSKY, *J. Polym. Sci. A-2* **4** (1966) 267.

126. *Idem, J. Appl. Phys.* **42** (1971) 4585.
127. H. A. DAVIS, *J. Polym. Sci. A-2* **4** (1966) 1009.
128. E. S. CLARK, *Soc. Plast. Eng. J.* **23**(7) (1967) 46.
129. Y. HASE and P. H. GEIL, *Polym. J.* **2** (1971) 560.
130. F. RYBNIKAR and P. H. GEIL, *J. Macromol. Sci.–Phys.* **B7** (1973) 1.
131. A. MEHTA and B. WUNDERLICH, *Makromol. Chem.* **175** (1974) 977.
132. G. MEINEL, A. PETERLIN and K. SAKAOKU, in "Analytical Calorimetry", edited by R. S. Porter and J. F. Johnson, (Plenum, New York, 1968) p. 15.
133. A. PETERLIN, *J. Polym. Sci. A-2* **7** (1969) 1151.
134. C. P. BUCKLEY, R. W. GRAY and N. G. McCRUM, *J. Polym. Sci. B* **7** (1969) 835.
135. E. W. FISCHER, H. GODDER and W. PIESCZEK, *J. Polym. Sci. C* **32** (1971) 149.
136. E. W. FISCHER, K. HAHN, J. KUFLER, U. STRUTH and R. BORN, *J. Polym. Sci., Polym. Phys. Ed.* **22** (1984) 1491.
137. S. NAGOU and K. AZUMA, *J. Macromol. Sci.–Phys.* **B16** (1979) 435.
138. H. H. KAUSCH and K. L. DEVRIES, *Int. J. Fract.* **11** (1975) 727.
139. K. ITOYAMA, *J. Polym. Sci., Polym. Phys. Ed.* **19** (1981) 1873.
140. R. POPLI and D. ROYLANCE, *Polymer. Eng. Sci.* **25** (1985) 828.
141. R. HOSEMANN, *J. Appl. Phys.* **34** (1963) 25.
142. B. WUNDERLICH, *Polymer* **5** (1964) 125.
143. D. J. BACON and N. A. GEARY, *J. Mater. Sci.* **18** (1983) 853.
144. N. A. GEARY and D. J. BACON, *ibid.* **18** (1983) 864.
145. D. J. BACON and K. THARMALINGAM, *ibid.* **18** (1983) 884.
146. A. W. THORNTON and P. PREDECKI, *J. Appl. Phys.* **41** (1970) 4266.
147. E. PIORKOWSKA and A. GALESKI, *J. Polym. Sci., Polym. Phys. Ed.* **23** (1985) 1723.
148. A. GALESKI, *ibid.* **19** (1981) 721.
149. P. B. BOWDEN and R. J. YOUNG, *J. Mater. Sci.* **9** (1974) 2034.
150. J. M. HAUDIN, in "Plastic Deformation of Amorphous and Semi-crystalline Materials", edited by B. Escaig and C. G'Sell (es éditions de Physique, Les Uas, France, 1982) p. 291.
151. P. H. GEIL, *J. Polym. Sci. A* **2** (1964) 3818.
152. A. PETERLIN, *J. Mater. Sci.* **6** (1971) 490.
153. H. H. KAUSCH, in "Advances in Polymer Science and Engineering", edited by K. A. Pae (Plenum, New York, 1972) p. 207.
154. B. W. CHERRY and P. L. McGINLEY, *Appl. Polym. Symp.* **17** (1971) 59.
155. A. W. AGAR, F. C. FRANK and A. KELLER, *Phil. Mag.* **4** (1959) 32.
156. V. F. HOLLAND, *J. Appl. Phys.* **35** (1964) 3235.
157. D. C. BASSETT, *Phil. Mag.* **10** (1964) 595.
158. M. L. WILLIAMS, *Ann. New York Acad. Sci.* **155** (1969) 539.
159. J. PETERMANN and H. GLEITER, *Phil. Mag.* **25** (1972) 813.
160. J. PETERMANN and R. M. GOHIL, *Polymer* **20** (1979) 596.
161. F. C. FRANK, A. KELLER and A. O'CONNOR, *Phil. Mag.* **3** (1958) 64.
162. H. D. KEITH and E. PASSAGLIA, *J. Res. Nat. Bur Stds* **68A** (1964) 513.
163. P. PREDECKI and W. O. STATTON, *Appl. Polym. Symp.* **6** (1967) 165.
164. L. G. SHADRAKE and F. GUIU, *Phil. Mag.* **34** (1976) 565.
165. *Idem, ibid.* **39** (1979) 785.
166. A. KELLER and J. G. RIDER, *J. Mater. Sci.* **1** (1966) 389.
167. T. HINTON and J. G. RIDER, *J. Appl. Phys.* **39** (1968) 4932.
168. L. A. SIMPSON and T. HINTON, *J. Mater. Sci.* **6** (1971) 558.
169. R. J. YOUNG, P. B. BOWDEN, J. M. RITCHIE and J. G. RIDER, *ibid.* **8** (1973) 23.
170. C. A. COULOMB, *Mem. Math. Phys.* **7** (1773) 343.
171. A. S. ARGON, R. D. ANDREW, J. A. GODRICK and W. J. WHILNEY, *J. Appl. Phys.* **39** (1968) 1899.
172. R. A. DUCKETT, S. RABINOWITZ and I. M. WARD, *J. Mater. Sci.* **5** (1970) 909.
173. P. B. BOWDEN and J. A. JUKES, *ibid.* **7** (1972) 52.
174. L. LIN, PhD thesis, MIT (1991).
175. U. F. KOCKS, A. S. ARGON and M. F. ASHBY, "Progress in Materials Science" Vol. 19, edited by B. Chalmers, J. W. Christian and T. B. Massaloki (Pergamon, Oxford, 1975) 110.
176. H. KIHO, A. PETERLIN and P. H. GEIL, *J. Polym. Sci.* **B3** (1965) 257.
177. I. L. HAY and A. KELLER, *Kolloid-Z. Z. Polym.* **204** (1965) 43.
178. D. P. POPE and A. KELLER, *J. Polym. Sci. Polym. Phys. Ed.* **13** (1975) 533.
179. A. KELLER and D. P. POPE, *J. Mater. Sci.* **6** (1971) 453.
180. I. L. HAY and A. KELLER, *ibid.* **2** (1967) 538.
181. *Idem, ibid.* **1** (1966) 41.
182. J. J. POINT, G. A. HOMES, D. GEZOVICH and A. KELLER, *ibid.* **4** (1969) 908.
183. D. P. POPE and A. KELLER, *ibid.* **9** (1974) 920.
184. *Idem, J. Polym. Sci., Polym. Phys. Ed.* **14** (1976) 821.
185. *Idem, J. Mater. Sci.* **12** (1977) 1105.
186. Z. H. STACHURSKI and I. M. WARD, *J. Macromol. Sci.–Phys.* **B3** (1969) 445.
187. H. GLEITER and A. S. ARGON, *Phil. Mag.* **24** (1971) 71.
188. A. COWKING and J. G. RIDER, *J. Mater. Sci.* **4** (1969) 1051.
189. F. C. FRANK, A. KELLER and A. O'CONNOR, *Phil. Mag.* **4** (1959) 200.
190. D. SHINOZABI and G. W. GROVES, *J. Mater. Sci.* **8** (1973) 1012.
191. J. J. POINT, M. DOSIERE, M. GILLIOT and A. GOFFIN-GERIN, *ibid.* **6** (1971) 479.
192. S. G. BURNAY, M. D. D. AERE and G. W. GROVES, *ibid.* **13** (1978) 639.
193. T. HINTON, J. G. RIGER and L. A. SIMPSON, *ibid.* **9** (1974) 1331.
194. D. A. ZAUKELIES, *J. Appl. Phys.* **33** (1962) 2797.
195. Y. TAJIMA, *J. Appl. Phys. Jpn.* **12** (1973) 40.
196. K. SHIGEMATSU, K. IMADA and M. TAKAYANAGI, *J. Polym. Sci. A-2* **13** (1975) 73.
197. G. E. ATTENBURROW and D. C. BASSETT, *J. Mater. Sci.* **14** (1979) 2679.
198. W. L. WU, V. F. HOLLAND and W. B. BLACK, *ibid.* **14** (1979) 250.
199. R. E. ROBERTSON, *J. Polym. Sci. A-2* **7** (1969) 1315.
200. W. ROSE and Ch. MEURER, *J. Mater. Sci.* **16** (1981) 883.
201. N. A. PERTSEV and V. I. VLADIMIROV, *J. Mater. Sci. Lett.* **1** (1982) 135.
202. S. J. DeTERESA, R. S. PORTER and R. J. FARRIS, *J. Mater. Sci.* **20** (1985) 1645.
203. F. C. FRANK and A. N. STROH, *Proc. Phys. Soc. B* **65** (1952) 811.
204. A. S. ARGON, in "Treatise of Material Science and Technology", edited by H. Herman (Academic, New York, 1972) p. 79.
205. T. ODA, S. NOMURA and H. KAWAI, *J. Polym. Sci. A* **3** (1965) 1993.
206. D. LEWIS, E. J. WHEELER, W. F. MADDAMS and J. E. PREEDY, *J. Polym. Sci. A-2* **10** (1972) 369.
207. P. PREDECKI and W. O. STATTON, *J. Appl. Phys.* **37** (1966) 4053.
208. *Idem, ibid.* **38** (1967) 4140.
209. J. M. PETERSON, *ibid.* **37** (1966) 4047.
210. R. J. YOUNG, *Phil. Mag.* **30** (1974) 85.
211. J. G. RIDER and K. M. WATKINSON, *Polymer* **19** (1978) 645.
212. W. P. LEUNG, F. C. CHEN, C. L. CHOY, A. RICHARDSON and I. M. WARD, *ibid.* **25** (1984) 447.
213. C. L. CHOY and W. P. LEUNG, *J. Polym. Sci. Polym. Phys. Ed.* **23** (1985) 1759.
214. H. CONRAD, *Mater. Sci. Eng.* **6** (1970) 265.
215. W. WU, A. S. ARGON and A. P. L. TURNER, *J. Polym. Sci., Polym. Phys. Ed.* **10** (1972) 2379.
216. M. BEVIS and E. B. CRELLIN, *Polymer* **12** (1971) 666.
217. B. A. BILBY and A. G. CROCKER, *Proc. Roy. Soc.* **A288** (1965) 240.

218. M. BEVIS and A. G. CROCKER, *ibid.* **A313** (1969) 509.
219. A. F. ACTON, M. BEVIS, A. G. CROCKER and N. D. H. ROSS, *ibid.* **A320** (1970) 101.
220. P. ALLAN, E. B. CRELLIN and M. BEVIS, *Phil. Mag.* **27** (1973) 127.
221. R. J. YOUNG and P. B. BOWDEN, *ibid.* **29** (1974) 1061.
222. H. KIHO, A. PETERLIN and P. H. GEIL, *J. Appl. Phys.* **35** (1964) 1599.
223. I. L. HAY and A. KELLER, *J. Polym. Sci. C* **30** (1970) 289.
224. T. SETO, T. HARA and K. TANAKA, *J. Appl. Phys. Jpn* **7** (1968) 31.
225. F. C. FRANK, V. B. GUPTA and I. M. WARD, *Phil. Mag.* **21** (1970) 1127.
226. D. LEWIS, E. J. WHEELER, W. F. MADDAMS and J. E. PREEDY, *J. Appl. Crystallogr* **4** (1971) 55.
227. J. R. WHITE, *J. Mater. Sci.* **9** (1974) 1860.
228. J. E. PREEDY and E. J. WHEELER, *ibid.* **12** (1977) 810.
229. P. ALLAN and M. BEVIS, *Phil. Mag.* **35** (1977) 405.
230. K. TANAKA, T. SETO and T. HARA, *J. Phys. Soc. Jpn* **17** (1962) 873.
231. R. H. PIERCE Jr, J. P. TORDELLA and W. M. D. BRYANT, *J. Amer. Chem. Soc.* **74** (1952) 282.
232. G. NATTA, *Makromol. Chem.* **16** (1955) 213.
233. E. R. WALTER and F. P. REDING, *J. Polym. Sci.* **21** (1956) 557.
234. W. R. SLICHTER, *ibid.* **21** (1956) 141.
235. P. W. TEARE and D. R. HOLMES, *ibid.* **24** (1957) 496.
236. A. TURNER-JONES, *ibid.* **62** (1962) S53.
237. Y. KIKUCHI and S. KRIMM, *J. Macromol. Sci.–Phys.* **B4** (1970) 461.
238. J. STEIDL and Z. PELZBAUER, *J. Polym. Sci. C* **38** (1972) 345.
239. H. KIHO, A. PETERLIN and P. H. GEIL, *J. Polym. Sci.* **B3** (1965) 157.
240. *Idem, ibid.* **3** (1965) 263.
241. A. COWKING, J. G. RIDER, I. L. HAY and A. KELLER, *J. Mater. Sci.* **3** (1968) 646.
242. K. KOBAYASHI and T. NAGASAWA, *J. Polym. Sci. C* **15** (1966) 163.
243. P. PREDECKI and A. W. THORNTON, *J. Appl. Phys.* **41** (1970) 4342.
244. R. G. C. ARRIDGE, *J. Mater. Sci.* **9** (1974) 155.
245. M. YAMADA, K. MIYASAKA and K. ISHIKAWA, *J. Polym. Sci., Polym. Phys. Ed.* **9** (1976) 1083.
246. R. G. QUYNN and H. BRODY, *J. Macromol. Sci.–Phys.* **B5** (1971) 721.
247. V. S. KUKSENKO and A. I. SLUTSKER, *Sov. Phys.–Solid State* **10** (1968) 657.
248. W. E. KAUFMAN and J. M. SCHULTZ, *J. Mater. Sci.* **8** (1973) 41.
249. J. PATERMANN and J. M. SCHULTZ, *ibid.* **13** (1978) 50.
250. A. J. OWEN and I. M. WARD, *ibid.* **6** (1971) 485.
251. E. S. CLARK, *J. Macromol. Sci.* **B4** (1970) 499.
252. R. G. QUYNN and H. BRODY, *J. Macromol. Sci.–Phys.* **B5** (1971) 721.
253. B. CAYROL and J. PETERMANN, *J. Polym. Sci., Polym. Phys. Ed.* **12** (1974) 2169.
254. E. S. CLARK, in "Structure and Properties of Polymer Films", edited by R. W. Leuz and R. S. Stein (Plenum, New York, 1973) p. 267.
255. G. W. GROVES and P. B. HIRSCH, *J. Mater. Sci.* **4** (1969) 929.
256. T. TAGAWA, *J. Polym. Sci., Polym. Phys. Ed.* **18** (1980) 971.
257. J. M. PETERSON and P. H. LINDENMEYER, *J. Appl. Phys.* **37** (1966) 4051.
258. R. S. STEIN, S. ONOGI, K. SASAGURI and D. A. KEEDY *ibid.* **34** (1963) 80.
259. K. SASAGURI, S. HOSHINO and R. S. STEIN, *ibid.* **35** (1964) 47.
260. A. PETERLIN and G. MEINEL, *Makromol. Chem.* **142** (1971) 227.
261. E. WEYNANT, J. M. HAUDIN and C. G.'SELL, *J. Mater. Sci.* **15** (1980) 2677.
262. T. T. WANG, *J. Polym. Sci., Polym. Phys. Ed.* **12** (1974) 145.
263. J. R. DRYDEN, A. S. DEAKIN and D. M. SHINOZAKI, *J. Mech. Phys. Solids.* **34** (1986) 81.
264. A. GALESKI, A. S. ARGON and R. E. COHEN, *Macromolecules* **21** (1988) 2761.
265. T. ODA, N. SAKAGUCHI and H. KAWAI, *J. Polym. Sci. C* **15** (1966) 223.
266. B. H. McCONKEY, M. W. DARLINGTON, D. W. SAUNDERS and C. G. CANNON, *J. Mater. Sci.* **6** (1971) 572.
267. Z. W. WILCHINSKY, *Polymer* **5** (1964) 271.
268. R. YANG and R. S. STEIN, *J. Polym. Sci. A-2* **5** (1967) 939.
269. K. SASAGURI, R. YAMADA and R. S. STEIN, *J. Appl. Phys.* **35** (1964) 3188.
270. T. ODA, N. SAKAGUCHI and H. KAWAI, *J. Polym. Sci. C* **15** (1966) 223.
271. R. S. MOORE, *J. Polym. Sci. A-2* **5** (1967) 711.
272. S. NOMURA, A. ASANUMA, S. SUEHIRO and H. KAWAI, *ibid.* **9** (1971) 1991.
273. S. NOMURA, M. MATSUO and H. KAWAI, *ibid.* **10** (1972) 2489.
274. D. Y. YOON, C. CHANG and R. S. STEIN, *ibid.* **12** (1974) 2091.
275. M. MATSUO, K. HIROTA, K. FUJITA and H. KAWAI, *Macromolecules* **11** (1978) 1000.
276. M. MATSUO, T. OGITA, S. SUEHIRO, T. YAMADA and H. KAWAI, *ibid.* **11** (1978) 521.
277. M. MATSUO, *J. Chem. Phys.* **72** (1980) 899.
278. R. J. ASARO, *Acta Metall.* **23** (1975) 1255.
279. G. MEINEL and A. PETERLIN, *J. Polym. Sci. A-2* **9** (1971) 67.
280. C. G'SELL and J. J. JONAS, *J. Mater. Sci.* **14** (1979) 583.
281. *Idem, ibid.* **16** (1981) 1956.
282. I. M. WARD, "Mechanical Properties of Solid Polymers", (Wiley-Interscience, London 1975) p. 275.
283. C. M. SARGENT and D. M. SHINOZAKI, *Scripta Metall* **11** (1977) 401.
284. N. IBRAHIM, D. M. SHINOZAKI and C. M. SARGENT, *Mater. Sci. Eng.* **30** (1979) 175.
285. D. M. SHINOZAKI and C. M. SARGENT, *ibid.* **35** (1978) 213.
286. C. M. SARGENT and D. M. SHINOZAKI, *ibid.* **43** (1980) 125.
287. J. DRYDEN, C. M. SARGENT and D. M. SHINOZAKI, *ibid.* **68** (1984) 73.
288. D. M. SHINOZAKI and C. M. SARGENT, *J. Mater. Sci.* **15** (1980) 1054.
289. D. M. SHINOZAKI, C. M. SARGENT and S. FEHR, *Mater. Sci. Eng.* **51** (1981) 93.
290. D. M. SHINOZAKI and C. M. SARGENT, *ibid.* **73** (1985) 77.
291. J. C. M. LI, *Canad. J. Phys.* **45** (1967) 493.
292. D. J. LLOYD and J. D. EMBURY, *Met. Sci. J.* **4** (1970) 6.
293. A. A. SOLOMON, C. N. AHQUIST and W. D. NIX, *Scripta Metall.* **4** (1970) 231.
294. A. S. ARGON, *Phil. Mag.* **28** (1973) 839.
295. R. N. HAWARD and G. THACKRAY, *Proc. Roy. Soc.* **A302** (1968) 453.
296. M. E. BOYCE, D. M. PARKS and A. S. ARGON, *Mech. Mater.* **7** (1988) 15.
297. J. M. PETERSON, *Polym. Sci. B* **7** (1969) 231.
298. T. K. CHAKI and J. C. M. LI, *J. Appl. Phys.* **56** (1984) 2392.
299. E. M. ARRUDA and M. BOYCE, *J. Mech. Phys. Solids* **41** (1993) 389.
300. L. A. DAVIS and C. A. PAMPILLO, *J. Appl. Phys.* **42** (1971) 4659.
301. C. A. PAMPILLO and L. A. DAVIS, *ibid.* **43** (1972) 4277.

Received 12 January 1993
and accepted 24 June 1993